



HORIZON 2020

HORIZON 2020 RESEARCH AND INNOVATION FRAMEWORK PROGRAMME OF THE EUROPEAN ATOMIC ENERGY COMMUNITY

Nuclear Fission and Radiation Protection 2018 (NFRP-2018-4)

Project acronym: **SANDA**
Project full title: **Solving Challenges in Nuclear Data for the Safety of European Nuclear facilities**
Grant Agreement no.: **H2020 Grant Agreement number: 847552**

Workpackage N°: **WP5**
Identification N°: **D5.9**
Type of document: **Deliverable**
Title: **Synthesis report on C/E validation and nuclear data trends**
Dissemination Level: **PP**
Reference: **UPM/SANDA20240719**
Status: **VERSION 1.0**

Comments:

	Name	Partner	Date	Signature
Prepared by:	N. García-Herranz	UPM	19-07-2024	
WP leader:	R. Jacqmin	CEA		
IP Co-ordinator:	E. González	CIEMAT		

LIST OF AUTHORS

Nuria García Herranz	UPM
Oscar Cabellos	UPM
Antonio Jiménez Carrascosa	UPM ¹
David Bernard	CEA/DES
Ivo Kodeli	UKAEA/JSI
Gašper Žerovnik	JSI
Steven van der Marck	NRG
Nicolas Leclaire	IRSN
Vicente Bécares	CIEMAT

ABBREVIATIONS AND ACRONYMS

EALF	Energy of the average lethargy causing fission
ICSBEP	International Criticality Safety Benchmark Evaluation Project
IRPHEP	International Reactor Physics Evaluation Project
JEFF	Joint Evaluated Fission and Fusion
LWR	Light Water Reactors
MOX	Mixed OXide
PIE	Post-Irradiation Experiments
PNFS	Prompt Fission Neutron Spectra
PWR	Pressurized Water Reactor
SEFOR	South-West Experimental Fast Oxide Reactor
SINBAD	Shielding Integral Benchmark Archive and Database
TOF	Time-of-Flight
TSL	Thermal Scattering Libraries
WPEC	Working Party on International Nuclear Data Evaluation Co-operation

¹ Paul Scherrer Institute (PSI) since March 2023.

EXECUTIVE SUMMARY

This deliverable of the EC SANDA project “Supplying Accurate Nuclear Data for Energy and non-Energy Applications” (H2020 Grant Agreement number 847552) addresses Task 5.2 “Validation studies using existing experiments”, Subtask 5.2.2 “*C/E* validation and trends”.

It compiles the findings of Deliverables 5.7 and 5.8 on validation of JEFF nuclear data files across reactor, shielding and criticality benchmarks as well as a validation of fission product nuclear data against MINERVE/CERES pile oscillation experiments, that was also envisaged in the task. As a result of the systematic benchmark calculations performed for each JEFF release, the needs for nuclear data improvement or reconsideration are synthesized, with particular indication of the benchmarks identified as useful for checking the performance of specific isotopes, reactions and energy ranges. Finally, new applications that should be addressed in future validation suites are proposed.

KEYWORDS

JEFF; nuclear data validation; criticality benchmarks; advanced fast reactors; thermal reactors; commercial PWR; shielding benchmarks; pile oscillation experiments, nuclear data trends and needs

Table of contents

LIST OF TABLES	2
LIST OF FIGURES	2
1. INTRODUCTION	3
2. NUCLEAR DATA TRENDS IN JEFF EVALUATIONS	4
2.1. C/E VALIDATION FOR FAST REACTORS	4
2.2. C/E VALIDATION FOR THERMAL REACTORS (INCLUDING COMMERCIAL LWRs).....	6
2.3. C/E VALIDATION FOR SHIELDING	8
2.4. C/E VALIDATION FOR CRITICALITY BENCHMARKS	10
2.5. C/E VALIDATION AGAINST MINERVE-CERES PILE OSCILLATION EXPERIMENTS	12
3. NEEDS OF C/E VALIDATION IN OTHER AREAS OF INTEREST	12
3.1. BENCHMARK BURNUP CREDIT – PHASE VII FOR SPENT FUEL CASKS.....	13
4. SUMMARY AND CONCLUSIONS	14
5. REFERENCES	15
6. ACKNOWLEDGEMENTS	15
7. DERIVED PUBLICATIONS	16
8. APPENDIX 1: VALIDATION OF FISSION PRODUCT DATA AGAINST MINERVE-CERES PILE OSCILLATION EXPERIMENTS	18
8.1. INTRODUCTION	18
8.2. MCNP MODELLING OF THE CERES EXPERIMENTS AT MINERVE.....	19
8.3. CALCULATIONS.....	21
8.3.1. EIGENVALUE DIFFERENCE METHOD (EVDM).....	21
8.3.2. PERTURBATION THEORY	26
8.3.3. MCNP KPERT CARD	27
8.4. CALCULATION RESULTS AND DISCUSSION	27
8.5. SUMMARY AND CONCLUSIONS.....	33
8.6. ACKNOWLEDGEMENTS.....	33
8.7. REFERENCES	33
8.8. ANNEX: ADJOINT FLUX CALCULATION WITH MCNP	34

List of Tables

Table 1. Nuclear data trends for JEFF derived from analysis of fast reactor benchmarks.	5
Table 2. Nuclear data trends for JEFF derived from analysis of thermal reactor benchmarks.	7
Table 3. Nuclear data trends for JEFF derived from analysis of shielding benchmarks (Part I).	8
Table 4. Nuclear data trends for JEFF derived from analysis of shielding benchmarks (Part II).	9
Table 5. Nuclear data trends for JEFF derived from analysis of criticality benchmarks (Part I - IRSN).	10
Table 6. Nuclear data trends for JEFF derived from analysis of criticality benchmarks (Part II - NRG).	10
Table 7. Conclusions of the analysis of MINERVE/CERES experiments.	12
Table 8. Values of keff of the MINERVE reactor with the oscillation sample density multiplied by several factors.	iError! Marcador no definido.
Marcador no definido.	
Table 9. Values of keff of the MINERVE reactor with the Sm7 sample density multiplied by several factors, for the ENDF/B-VII.1 and the JEFF-3.3 libraries.	iError! Marcador no definido.
Table 10. EVDM results (MCNP6.2 and ENDF/B-VII.1) vs. experimental measurements.	iError! Marcador no definido.
Table 11. EVDM results (MCNP6.2 and JEFF-3.3) vs. experimental measurements.	iError! Marcador no definido.
Table 12. Perturbation theory vs. experimental measurements.	iError! Marcador no definido.
Table 13. KPERT results (MCNP6.2 and ENDF/B-VII.1, 10 inactive cycles).	iError! Marcador no definido.
Table 14. Total neutron production in the MINERVE system	36

List of Figures

Figure 1. Comparison of JEFF-4T2.2 in BUC/Phase-VII Benchmark.	13
Figure 2. Comparison of JEFF-4T2.3 and ENDF/B-VIII.1b2 in BUC/Phase-VII Benchmark.	14
Figure 3. Schematics of the MINERVE reactor in the CERES configuration.	20
Figure 4. Detail of the oscillation sample.	20
Figure 5. Neutron spectra in MINERVE/CERES sample position with the reference UO ₂ sample (UF) and a samples containing ¹⁴⁷ Sm (Sm7) and ¹⁴⁹ Sm (Sm9).	21
Figure 6. Gain in computer time with the variant of the EVDM method implemented in this work.	23
Figure 7. $\Delta\rho$ vs. density for Nd (nat), Nd143 and Nd145 samples.	23
Figure 8. $\Delta\rho$ vs. density for Sm (nat), Sm149, Sm147 and Sm152 samples. Notice the different range of density increases for the case of Sm-147.	24
Figure 9. $\Delta\rho$ vs. density for Gd155, Eu153 and Rh103 samples.	24
Figure 10. $\Delta\rho$ vs. density for Cs133, Mo95 and Tc99 samples.	24
Figure 11. EVDM results (MCNP6.2 and ENDF/B-VII.1) vs. experimental measurements.	29
Figure 12. EVDM results (MCNP6.2 and JEFF-3.3) vs. experimental measurements.	30
Figure 13. Perturbation theory vs. experimental measurements.	31
Figure 14. KPERT results (MCNP6.2 and ENDF/B-VII.1) vs. experimental measurements.	32
Figure 15. Calculated adjoint flux spectrum in the simple cell (UF) at two different levels of subcriticality. APOLLO2 results [Santamarina 2016] are also plotted for comparison.	36

1. Introduction

Nuclear data validation is crucial to support the calculation-based decision-making in nuclear applications. This validation process involves using integral experiments to assess the accuracy of an evaluation in representing experimental measurements.

A wide range of integral experiments encompassing criticality, reactor physics, and radiation shielding —available in international databases such as ICSBEP, IRPhEP, and SINBAD, as well as in other legacy sources—, have been utilized in SANDA project Deliverables D5.7 [García-Herranz, 2024] and D5.8 [Leclaire, 2022] to contribute to the validation of JEFF nuclear data files, up to JEFF-4T3 evaluation. In the deliverables, the validation for the entire JEFF-x libraries with a large number of experiments involving many nuclides and reactions have allowed to make global statements about the quality of JEFF libraries. On the other hand, the validation for individual nuclear data, where individual impacts have been sought by using selected sets of integral experiments, have allowed to further investigate the reasons of biases and infer trends. Additionally, the comparison of the JEFF-x performance with other libraries (e.g. ENDF/B-x or JENDL-x) have allowed to identify differences in the nuclear data that have to be reviewed. All of this has enabled iterative improvements of JEFF data.

This report aims at extracting useful conclusions about nuclear data trends and needs of nuclear data review (and possibly improvement) in JEFF evaluations. Two considerations emerge that justify comparing the findings obtained in Deliverables D5.7 and D7.8 where different experiments were used:

- The predictive capability of an evaluation may be accurate enough within a specific application domain but not in others, while the same data is intended to support a variety of applications.
- Not all application domains were addressed in D5.7 and D5.8, so it seems advisable to identify additional areas of interest for future consideration.

Hence, this deliverable aims to synthesize and analyse the findings of the work conducted under SANDA Task 5.2 trying to draw unambiguous conclusions regarding the nuclear data status in JEFF libraries across all validation domains examined in this task, as well as highlighting other domains of interest for validation.

The report is structured as follows. First, in section 1, the needs for improvement for the specific nuclear data found relevant in D5.7 and D5.8 are given, indicating the specific application where that reaction was detected to be responsible of the biases. Findings highlighted by the MINERVE/CERES pile oscillation experiments are also compiled in this section. The data supporting those conclusions can be found in the mentioned deliverables or in the Appendix section. This way, conclusions derived for each application can be compared. Then, in section 3, other application domains that can be useful to identify nuclear data trends are presented. Finally, this report concludes with a summary and conclusions, and a list of related publications.

2. Nuclear data trends in JEFF evaluations

2.1. C/E validation for fast reactors

Nuclear data validation using IRPhEP fast-spectrum benchmarks (EALF ranging from 0.11 MeV to 0.36 MeV, with sensitivities significant in the URR range) and SEFOR experiments allowed for the following conclusions. Main findings are presented in Table 1.

- C-E deviations for multiplication factor k -eff (Mean Absolute Deviation ~ 300 pcm) for both JEFF-3.3 and JEFF-4T3 are covered by the JEFF-3.3 nuclear data-induced uncertainties, mainly due to the large impact of nuclear data uncertainties in fast spectrum region (around 1000 pcm).
- Regarding multiplication factor k -eff, JEFF-4T3 improves biases with respect to JEFF-3.3 but overestimates in general the benchmark values and calculations do not align with benchmarks within one experimental benchmark standard deviation, which is nearly achieved with ENDF/B-VII.1.
- The main contributors to k -eff deviations of JEFF-4T3 with respect to ENDF/B-VII.1 are ^{239}Pu and ^{238}U isotopes, with many opposite contributions:
 - JEFF-4T3 ^{239}Pu with respect to ENDF/B-VII.1 leads to an increase of k -eff driven mainly by (n,f) and a decrease driven by $\bar{\nu}$ (nubar). PNFS data is also relevant as well as elastic angular distribution. Perturbation of inelastic scattering angular distribution does not seem to have a significant impact.
 - JEFF-4T3 ^{238}U with respect to ENDF/B-VII.1 leads to an increase of k -eff driven by (n,f) and (n,γ) , while important perturbations are introduced by the elastic scattering cross section and the elastic angular distribution between 0.1 and 1 MeV. These effects have opposite signs and consequently compensate for each other. Perturbation of inelastic scattering angular distribution does not seem to have a significant impact.
- Analysis of the elastic scattering angular distributions in JEFF-4T3 is suggested. The computation of sensitivities to P_1 (and higher P_N term) angular scattering is recommended to identify potential deviations in experiments that are strongly sensitive to angular distributions. It would be very useful to incorporate the capability to compute deviations in P_N (at least P_1) angular scattering between two libraries into the NEA's NDaST tool.
- Regarding sodium void cases, JEFF-4T3 exhibits a better agreement to benchmark values than JEFF-3.3. With JEFF-3.3, C-E biases progressively increased as more sodium was voided; this trend no longer occurs with JEFF-4T3, indicative of an improvement of ^{239}Pu cross sections around 1 keV.
- Regarding control rod worths, a large uncertainty is associated to the experimental measurements so that the C-E discrepancies are covered by the 1σ experimental uncertainties and no useful information can be derived.

Table 1. Nuclear data trends for JEFF derived from analysis of fast reactor benchmarks.

General comments		
<ul style="list-style-type: none"> • JEFF-4T3 improves C-E biases with respect to JEFF-3.3 but overestimates benchmark values. ENDF/B-VII.1 exhibits in general a better agreement. • ^{239}Pu and ^{238}U data are main responsible of the biases, with many opposite contributions. 		
Reaction	Energy range	Benchmark where the reaction contributes significantly to C/E biases or differences to other libraries
$^{238}\text{U} (n,n)$	0.1 MeV - 1 MeV	k-eff of SNEAK reactors from IRPhEP. Impact of those reactions using JEFF-3.3 or JEFF-4T3 differs significantly from using ENDF/B-VII.1 or ENDF/B-VIII.0. The same effects observed in the FLATTOP benchmarks (FLATTOP-U ²³³ , FLATTOP-U ²³⁵ , FLATTOP-Pu ²³⁹)
^{238}U elastic angular distribution		
$^{238}\text{U} (n,\gamma)$	~ 1 keV	Doppler effect of SEFOR reactor. It allowed to identify a typo for the 808 eV p-wave Γ_g parameter in JEFF-3.3. New JEFF-4T3 exhibits a good agreement with experimental values
	20 keV - 820 keV	k-eff of fast-spectrum ICSBEP benchmarks. Responsible of differences between JEFF-3.3 and JEFF-3.1.1
$^{239}\text{Pu} (n,\gamma)$	~ 1 keV	Sodium void worth of ZPPR-12 or ZPPR-2 from IRPhEP. Contributor to differences between JEFF-3.3 and JEFF-3.1.1. JEFF-4T3 exhibits a significant better agreement with experimental values
$^{239}\text{Pu} (n,f)$	~ 1 keV	Sodium void worth of ZPPR-12 or ZPPR-2 from IRPhEP exhibits large sensitivity in this energy range
	~ 100 keV	k-eff of MOX-fueled reactors like ZPPR from IRPhEP exhibits large sensitivity in this energy range
$^{23}\text{Na} (n,\gamma)$	2 keV – 200 keV	Sodium void reactivity (SVR) of ZPPR-12 or ZPPR-2 from IRPhEP exhibits significant sensitivities in these energy ranges. Contributors to differences in SVR prediction between JEFF-3.3 and JEFF-3.1.1
$^{23}\text{Na} (n,n)$	Above 2 keV	
$^{23}\text{Na} (n,n')$	Above 0.5 MeV	
$^{58}\text{Ni} (n,n)$	0.1 MeV - 1 MeV	k-eff of FFTF reactor from IRPhEP (inconel-reflected core) exhibit large sensitivities to this reaction. JEFF-4T3 agrees extremely well to experimental values

2.2. C/E validation for thermal reactors (including commercial LWRs)

Nuclear data validation for thermal reactors, both experimental and commercial LWRs, allowed for the following conclusions. Main findings are presented in Table 2.

Validation using IRPhEP KRITZ and CREOLE thermal reactor benchmarks showed that:

- For KRITZ-LWR-RESR-001, -002 and -003, performance of JEFF-3.3 is better for UO₂ cases than for the MOX case. Large C-E biases at room and elevated temperatures are found for the MOX case, for both JEFF-3.3 and ENDF/B-VIII.0.
- For KRITZ-LWR-RESR-004, C-E biases for JEFF-3.1.1 and ENDF/B-VII.1 are very similar (from 400 to 600 pcm) and no trend with temperature is observed, being results consistent with other thermal spectrum low-enriched uranium benchmarks. Although C-E deviations with JEFF-3.3 are smaller than for JEFF-3.1.1, they exhibit a strong trend with temperature for Series 4. This strong trend may indicate remaining nuclear data biases in JEFF-3.3. A detailed perturbation analysis allowed to conclude that this trend effect is mainly dominated by the ²³⁵U(n,fission) cross section in the energy range ~ 0.01 eV – 1eV. Changes between 0.05eV and 0.1eV in JEFF-3.3 with respect to JEFF-3.1.1 or ENDF/B-VII.1 impact significantly Series 4 benchmark results.
- For CREOLE benchmarks, the trends with temperature of C-E deviations in temperature reactivity effect are small (less or equal to 0.24 pcm/°C) for JEFF-3.3 and even lower for JEFF-4T3 (less or equal to 0.17 pcm/°C).

Analysis of Post-Irradiation Experiments (PIE) of PWR reprocessed UO₂ pellets showed that while JEFF-4T3 C/E isotopic prediction is consistent with experimental uncertainties, trends with burnup were observed. A perturbation analysis suggested that some capture cross sections in specific energy regions of the thermal range should still be revised:

- JEFF-4T3/²³⁹Pu(n_{[0.10-0.53]eV},γ) should be increased by (+5.3±1.4)% (prior uncertainty was ±3%).
- JEFF-4T3/²⁴⁰Pu(n_{[0.53-4.00]eV},γ) should be increased by (+1.5±2.2)% (prior uncertainty was ±3%).

Finally, analysis of the C-E biases in the critical boron letdown curve for a typical 3-loop 1000 MWe Westinghouse-type PWR for different consecutive cycles were performed. Nuclear data quality directly impacts on the reactivity prediction, core power distribution, fuel peaking factors, cycle length, fuel efficiency, etc., resulting in overly conservative margins, i.e., power plant economic underperformance. The analysis showed that:

- Even if for JEFF-3.3 the C-E bias is within ±50 ppm, which is the acceptance criteria for PWR reactors, a trend along burnup can be observed. JEFF-3.3 predicts a higher loss of reactivity along burnup than ENDF/B-VII.1, mainly due to the differences in the evaluation of ²³⁹Pu, being the impact of ²³⁸U and ²³⁵U evaluations also significant.
- For JEFF-4T2.2, the loss of reactivity with burnup with respect to ENDF/B-VII.1 was even more pronounced than for JEFF-3.3; it can be attributed mainly to ²³⁹Pu and ²³⁵U, while the impact of ²³⁸U seems to be quite small. At high burnup, contribution of fission products can be also at the origin of discrepancies.
- For JEFF-4T3, a larger reactivity loss along burnup is still predicted compared to ENDF/B-VII.1, ENDF/B-VIII.0 and ENDF/B-VIII.1b2, although lower than for JEFF-4T2.2. Such wrong prediction of reactivity along burnup severely limits the use of JEFF-4.x evaluations in Light Water Reactor (LWR) analysis. The most influential nuclides (nuclear data) are ²³⁹Pu, ²⁴⁰Pu, ²⁴¹Pu, ²³⁵U and ²³⁸U, as well as the fission yields of a few critical fission products and their capture cross-sections. Additional studies are urgently needed to address these nuclear data shortcomings.

- Fuel assembly calculations proved useful in assessing reactivity differences along burnup with lower computational expense, and in identifying whether more effort for JEFF-4.x is necessary to address this burnup issue in LWRs. An analysis of a typical PWR Westinghouse 17x17 fuel assembly at 4.8 w/o as a function of burnup allowed us to observe changes in reactivity isotope-by-isotope. For example, a significant increase in reactivity was observed with the new ²⁴¹Pu evaluation in ENDF/B-VIII.1b2, whereas this isotope did not play a significant role in the loss of reactivity in ENDF/B-VIII.0.

Table 2. Nuclear data trends for JEFF derived from analysis of thermal reactor benchmarks.

Reaction	Energy range	Benchmark where the reaction contributes significantly to C/E biases or differences to other libraries
²³⁹ Pu (n,γ) and ²³⁹ Pu (n,f)	0.01 eV - 0.10 eV	KRITZ-2:19 (KRITZ-LWR-RESR-001) from IRPhEP. Large biases for JEFF-3.3 that increase with temperature, and reduce when using ²³⁹ Pu from ENDF/B-VIII.0
²³⁹ Pu (n,γ)	0.10 eV - 0.53 eV	Post-Irradiation Experiments of PWR reprocessed UO ₂ pellets. JEFF-4T3 reaction in this energy range should be increased by (+5.3±1.4)% (prior uncertainty was ±3%)
²⁴⁰ Pu (n,γ)	0.53 eV - 4.00 eV	Post-Irradiation Experiments of PWR reprocessed UO ₂ pellets. JEFF-4T3 reaction in this energy range should be increased by +1.5 or ±2.2% (prior uncertainty was ±3%)
²³⁵ U (n,f)	0.05 eV - 0.10 eV	KRITZ-4 (KRITZ-LWR-RESR-004) from IRPhEP exhibits strong trends with temperature mainly dominated by this reaction in this energy range.
²³⁵ U, ²³⁸ U, ²³⁹ Pu, ²⁴⁰ Pu, ²⁴¹ Pu and Fission Products (fission yields and capture cross-sections)		Measurements for actual PWR soluble boron letdown curves. A significant C/E bias in reactivity observed with JEFF-3.3 and JEFF-4T2.2. Although biases are lower in the case of JEFF-4T3, a reactivity loss along burnup larger than expected is still predicted compared to ENDF/B-VII.1, ENDF/B-VIII.0 and ENDF/B-VIII.1b2. Despite the accumulated feedback from many years of LWR operation, the latest JEFF-4.x data still have issues, which affect fuel depletion and reactivity predictions. Therefore, improvements are needed for the indicated actinides cross sections. Moreover, for reactor transients, improvements are needed in short-lived neutron-absorbing fission product yields and cross sections.

2.3. C/E validation for shielding

Nuclear data validation using different shielding and transmission benchmarks from SINBAD and ICSBEP was performed. They exhibit high sensitivity to neutron leakage, so they were especially useful for testing scattering (elastic and inelastic) cross sections and angular distributions. The analysis performed led to the conclusions presented in Table 3 and Table 4.

Table 3. Nuclear data trends for JEFF derived from analysis of shielding benchmarks (Part I).

Reaction	Energy range	Benchmark where the reaction contributes significantly to C/E biases or differences to other libraries
Fe evaluation: reaction rates in $^{27}\text{Al} (n,\alpha)$		<ul style="list-style-type: none"> • Reaction rates measured in ASPIS Iron-88 benchmark. Worse C/E agreement using JEFF-3.3 and ENDF/B-VIII.0 compared to older iron evaluations (reaction rates were severely overestimated). • PCA and PCA Replica benchmarks showed good reaction rates C/E agreement using JEFF-3.3 and ENDF/B-VIII.0 (or slightly underestimated). • The different behavior between ASPIS-Iron88 and PCA may be due to systematic uncertainties in ASPIS measurements • Considerable improvements at all energies using JEFF-4T evaluations.
Fe evaluation: reaction rates in $^{32}\text{S} (n,p)$		<ul style="list-style-type: none"> • Reaction rates measured in ASPIS Iron-88 and PCA Replica benchmarks. Worse C/E agreement using JEFF-3.3 and ENDF/B-VIII.0 was observed compared to older iron evaluations. • PCA and PCA Replica results consistent with ASPIS. • Considerable improvements at all energies using JEFF-4T evaluations.
Fe evaluation: reaction rates in $^{115}\text{In} (n,n')$, $^{103}\text{Rh} (n,n')$, $^{197}\text{Au} (n,\gamma)$		<ul style="list-style-type: none"> • Reaction rates measured in ASPIS Iron-88 and PCA Replica benchmarks. Good agreement in the measured reaction rates for fast, intermediate and thermal neutron energies using JEFF-4T evaluations, with C/E values close to, or within 1σ experimental uncertainties.
KFK γ -ray leakage benchmark		<ul style="list-style-type: none"> • Relatively high experimental uncertainties allow only a generic overall verification of the neutron and gamma spectra using these older benchmark. Suggestion to repeat these measurements using modern techniques;
CIAE Iron slab benchmark		<ul style="list-style-type: none"> • Analysis pinpoints possible inconsistencies in angular distributions (backward scattering).

Table 4. Nuclear data trends for JEFF derived from analysis of shielding benchmarks (Part II).

Reaction	Energy range	Benchmark where the reaction contributes significantly to C/E biases or differences to other libraries
Elastic and inelastic cross sections and angular distributions of beryllium, graphite, iron, Li ₂ O, N ₂ , O ₂ , lead	0.1 MeV – 14 MeV	<ul style="list-style-type: none"> • Analysis of the angular neutron leakage spectra in JAEA Fusion Neutron Source (FNS) Time-of-Flight (TOF) experiments.
Elastic and inelastic cross sections and angular distributions of Zr, Al, Mo, Cu, W, Co, Ti, teflon, Si, Nb, Mn, Cr, LiF, As	0.1 MeV – 14 MeV	<ul style="list-style-type: none"> • Analysis of the angular neutron leakage spectra in OKTAVIAN Time-of-Flight benchmarks from SINBAD • Poor performance identified for some elements when comparing JEFF-3.3, JEFF-4T2 with ENDF/B-VII.1, ENDF/B-VIII.1 and experimental data. • New evaluation of Cu in JEFF-4T3 and ENDF/B-VIII.b3 significantly improved C/E biases. [Capote, 2024]
²³⁵ U (n, total) and ²³⁵ U (n, f)	10 eV – 20 keV	<ul style="list-style-type: none"> • Neutron transmission experiments ICSBEP/FUND-JINR-1/E-MULT-TRANS-001 useful to assess the self-shielding for the ²³⁵U total and fission transmission. • JEFF-3.3 and JEFF-4T0 behaves similar than ENDF/B-VII.1 and ENDF/B-VIII.0 compared to experimental data. • Good C/E agreement for the total transmission function at low ²³⁵U atom densities, worsening at higher densities. • Poor C/E agreement for the fission transmission function at low ²³⁵U atom densities, that improves at higher densities.

2.4. C/E validation for criticality benchmarks

Nuclear data validation using a large set of criticality benchmarks, assumed to cover a wide range of cases in terms of fissile media and energy spectra², was presented in Deliverable D5.8. A total of 576 benchmark cases was selected by NRG and 182 benchmark cases by IRSN, being 120 benchmark cases common. Nuclear data files were generated separately by IRSN and NRG using the NJOY code. Main findings are presented in Table 5 and Table 6.

Table 5. Nuclear data trends for JEFF derived from analysis of criticality benchmarks (Part I - IRSN).

General comments		
<ul style="list-style-type: none"> In general, k-eff results with recent evaluations (JEFF-33, JEFF-4T2, ENDF/B-VIII.0) are in good agreement with benchmark values considering experimental uncertainty margins. 		
Reaction	Energy range	Benchmark where the reaction contributes significantly to C/E biases or differences to other libraries
¹⁶ O, ²³⁵ U and ²³⁸ U, TSL of water		<ul style="list-style-type: none"> New evaluations can explain discrepancies between the JEFF-3.3 and ENDF/B-VIII.0 in thermal energy range.
Nickel		<ul style="list-style-type: none"> New evaluation of nickel in JEFF-4T1 leads to strong overestimation of k-eff that is not realistic.
⁵⁶ Fe	Epithermal range	<ul style="list-style-type: none"> JEFF-3.3 and JEFF-4T1 evaluations lead to k-eff values that are further from the benchmark values compared with the ENDF/B-VIII.0 evaluation of ⁵⁶Fe.
⁶³ Cu, ⁶⁵ Cu and ²³⁵ U, ²³⁸ U		<ul style="list-style-type: none"> JEFF-3.3 evaluation of those isotopes tends to improve k-eff results for the ZEUS experiments compared with ENDF/B-VIII.0.

Table 6. Nuclear data trends for JEFF derived from analysis of criticality benchmarks (Part II - NRG).

Material	Spectrum	Comments
Uranium	Thermal spectrum	<ul style="list-style-type: none"> JEFF-4T2 and JEFF-3.3 exhibit a good C/E agreement for benchmarks with (almost) only uranium and water. In cases where there is a slight trend of the C/E values as a function of the pitch of the lattice (or another parameter that influences the neutron spectrum), the trend for JEFF-4T2 is never higher than for JEFF-3.3.
	Fast spectrum	<ul style="list-style-type: none"> JEFF-4T2 performs similarly to JEFF-3.3, JEFF-4T1 and ENDF/B-VIII.0 for benchmarks with (almost) only uranium. A trend in C/E values with EALF appears for several HEU benchmarks. It is unclear whether this trend, observed across all libraries, is caused by the benchmarks themselves or by the nuclear data.
Plutonium	Fast spectrum	<ul style="list-style-type: none"> JEFF-3.3 and JEFF-4T1 exhibit a good C/E agreement in general considering the uncertainty margins.

² The benchmarks were chosen so that they could exhibit sufficient sensitivity of k_{eff} to the nuclear data that the benchmark was assumed to validate. Benchmarks exhibiting too high uncertainties or unexplained uncertainties were systematically discarded from the selection.

		<ul style="list-style-type: none"> • For cases with no good agreement, the deviation can be attributed to the nuclear data of the reflector material (aluminum and nickel in JEFF-4T1).
Reflectors	Thermal spectrum	<ul style="list-style-type: none"> • JEFF results exhibit a C/E good agreement in general considering the uncertainty margins. • For steel or nickel reflectors, a slight trend of C/E with increasing reflector thickness can be identified for LEU-COMP-THERM-088. • For lead reflectors, LEU-COMP-THERM-010 and -017 show an influence of the distance between the lead reflector and the fuel array on C/E results.
	Fast spectrum	<ul style="list-style-type: none"> • JEFF-4T1 data for Al, V, Ti, and Ni are not reliable. • JEFF-4T2 improved data for Al, Ti, and Ni. • For V the trend of C/E values with increasing reflector thickness is roughly the same for all libraries. • For other materials, e.g. beryllium, graphite, depleted uranium, etc., the results are in good agreement with the benchmark values considering the uncertainty margins.
Absorbers		<ul style="list-style-type: none"> • JEFF-3.3, JEFF-4T1, JEFF-4T2, JEF2.2, ENDF/B-VIII.0 exhibit a trend with the concentration of the absorber element in solution (gadolinium, boron and cadmium) for several benchmarks. • HEU-MET-FAST-007 (cases 32-34) and LEU-COMP-THERM-033 strongly improved when using JEFF-4T2 data for fluorine.
Temperature effect		<ul style="list-style-type: none"> • Kritz-4 benchmark with analysis of temperature effect between 20.4 °C and 245.8 °C (U(1.35%)O₂ rods in borated water) : positive trend of C-E for JEFF-3.3 with increasing temperature, up to almost 1 pcm/°C. This trend is similar in JEFF-4t1 results, but smaller in ENDF/B-VIII.0 results. • Creole benchmark with U(3.1%)O₂ and UO₂-PuO₂ rods : results show significantly smaller trends, the absolute values of which are smaller than 0.25 pcm/°C for all libraries for all four core configurations of Creole.

2.5. C/E validation against MINERVE-CERES pile oscillation experiments

An additional validation study also performed under SANDA Task 5.2 is the analysis of integral measurements of fission product nuclear data in the MINERVE/CERES experiments that are available in IRPhE [Becares, 2024].

In these experiments, a small sample is introduced in a critical reactor core, which becomes slightly subcritical or supercritical as the result of this perturbation. Then the reactor is returned to a critical state by means of the adjustment of a control rod, and from the magnitude of this adjustment the impact on the reactivity can be inferred.

However, since the reactivity introduced by the sample is small (a few pcm), Monte Carlo calculation of this reactivity difference is cumbersome, as the statistical uncertainties mask the results when they are calculated as simple differences of k_{eff} between configurations (referred as EigenValue Difference Method, or EVDM). Hence, perturbative calculations are preferred, but these techniques bring another disadvantages (approximations, need to perform adjoint-weighted calculations). For this reason, under CHANDA Task 12.1 a variant of the EVDM method was developed to allow Monte Carlo evaluation of these small reactivity differences. This technique has been applied, alongside with perturbation calculations, to analyse the aforementioned MINERVE/CERES oscillation experimental data. Main findings are summarized in Table 7. Complete results are presented in detail in the Appendix 2.

Table 7. Conclusions of the analysis of MINERVE/CERES experiments.

General comments		
<ul style="list-style-type: none"> Reactivity oscillation experiments at MINERVE/CERES for a series of relevant fission products analyzed (MCNP-6.2 code) with the EigenValue Difference Method (EVDM) and the adjoint-weighted perturbation theory 		
Isotope	Spectrum	Results
^{NAT} Sm, ¹⁴⁹ Sm, ¹⁴⁷ Sm, ¹⁵² Sm, ^{NAT} Nd, ¹⁵³ Nd, ¹⁵⁵ Nd, ¹⁵⁵ Gd, ¹⁵³ Eu, ¹⁰³ Rh, ¹³³ Cs, ⁹⁵ Mo, ⁹⁹ Tc	MINERVE/CERES reactor spectrum (see Figure 8 in Appendix 1)	<ul style="list-style-type: none"> C/E ratios within approx. $\pm 10\%$ No significant difference between nuclear data libraries (ENDF/B-VII.1, ENDF/B-VIII.0, JENDL-5, JEFF-3.3, JEFF-4T1, JEFF-4T2, JEFF-4T3)

3. Needs of C/E validation in other areas of interest

Some benchmarking activities conducted without experimental data can be useful for detecting potential deteriorations of nuclear data and highlighting applications where more nuclear data validation efforts are needed.

One of these exercises is the OECD/NEA Burn-up Credit Criticality Safety Benchmark – Phase VII, that was used to assess JEFF-4.x nuclear data for spent fuel casks (see section 3.1).

Apart from spent fuel casks, other applications of interest for the benchmarking of JEFF evaluations prior to a final release of evaluated files were identified:

- Ex-core calculations for assessment of neutron fluence and displacements per atom. Accurate prediction of the neutron fluence in the Reactor Pressure Vessel (RPV) is receiving more and more attention with the life extension of the operating fleet of Light Water Reactors as it is key in the radiation-induced embrittlement. Therefore, ex-core benchmarking of Nuclear Data (e.g ¹⁶O and ⁵⁶Fe nuclear data, jointly with the angular distribution of inelastic scattering) is a relevant

activity to be performed to detect potential deteriorations in the performance for this type of applications.

- Depletion calculations to assess the potential reactivity changes with burnup using SFCOMPO benchmarks.
- Another relevant application where nuclear data needs should be explored is proton-therapy centres. The activation of mechanical elements (such as accelerators and beam parts), ambient (air, water, ground), and shielding is a relevant issue, linked with safety radiation protection, as well as with the future dismantling and management of radioactive materials produced along the operation.

3.1. Benchmark Burnup Credit – Phase VII for spent fuel casks

The computational OECD/NEA Burn-up Credit Criticality Safety Benchmark – Phase VII (BUC/Phase-VII) [Radulescu, 2012], defined within the OECD/NEA Expert Group on Burnup Credit Criticality Safety, was used to test the performance of JEFF-4.x nuclear data evaluations in transport packages.

The benchmark consists of a 3D cask for 21 fresh 17x17 fuels assemblies at 4.5 w/o at room temperature. Specifications can be found in [Radulescu, 2012]. A total of 13 organizations participated in the benchmark using different criticality codes and nuclear data libraries. The mean value of the participants’ k-eff results for the representative fuel cask was 1.1485. The lower and upper bands representing the standard deviation values of the participants’ k-eff results were ± 260 pcm.

Criticality calculations were performed previously for JEFF-3.3 and ENDF/B-VIII.0 nuclear data [Plompen, 2020] and k-eff values compared with those available in the benchmark. Now, recent JEFF-4.x evaluations were employed in MCNP6.1 calculations.

Figure 1 shows a comparison of k-eff results for JEFF-4T2.2 [Cabellos, 2022] and Figure 3 for JEFF-4T3 and ENDF/B-VIII.1b2 [Cabellos, 2023]. It can be observed that those beta evaluations exhibit an excellent agreement with the mean value of the participant’s k-eff results and other nuclear data evaluations.

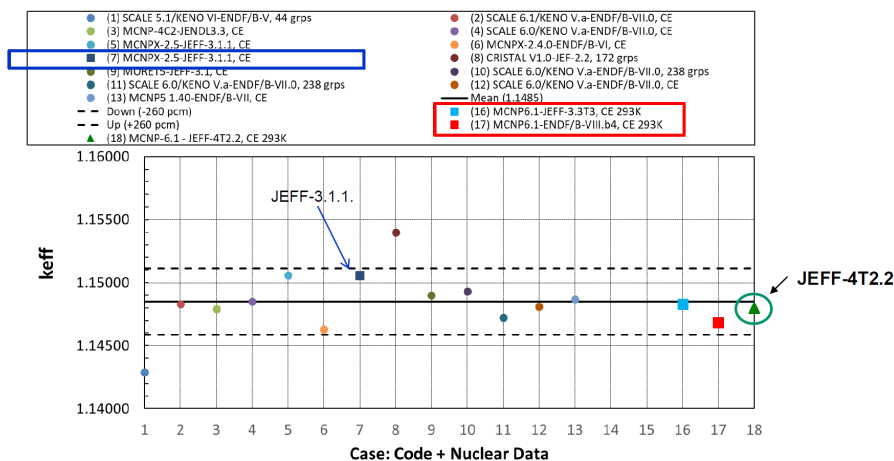


Figure 1. Comparison of JEFF-4T2.2 in BUC/Phase-VII Benchmark.

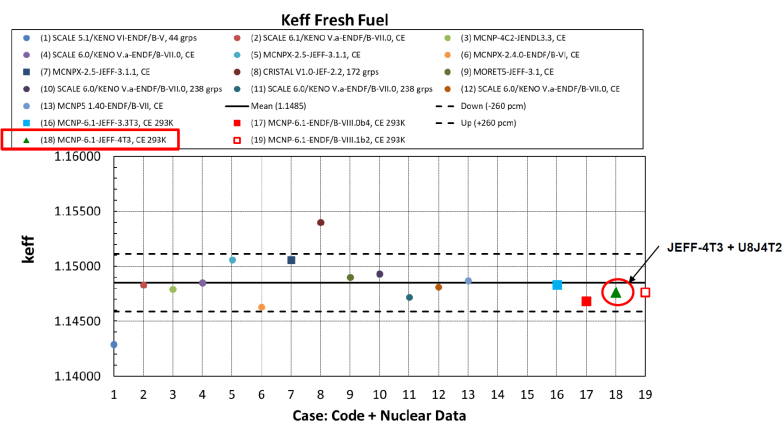


Figure 2. Comparison of JEFF-4T2.3 and ENDF/B-VIII.1b2 in BUC/Phase-VII Benchmark.

4. Summary and Conclusions

Validation assesses the predictive capability of a nuclear data evaluation within a specific application domain using available observations. In the SANDA project, a set of integral experiments from criticality, reactor physics, and shielding experimental databases have been utilized for nuclear data validation, including various types of measurements such as k-eff, reactivity coefficients, and reaction rates.

Extracting useful conclusions about specific nuclear data from the use of integral experiments is highly complex, even if methodological errors can be neglected in practice using Monte Carlo methods. This complexity arises from various factors. Firstly, experiments typically involve numerous isotopes and reactions (fission, capture, scattering, etc.) with correlated data. Secondly, there are multiple phenomena within the computational framework not directly related to nuclear data, such as geometry configuration and physical conditions, which impact the measured values. As a result, compensating effects come into play, presenting a significant challenge in drawing unambiguous conclusions about nuclear data needs.

Validation with criticality experiments, assumed to cover a wide range of cases in terms of fissile media and energy spectra, allowed identify main tendencies in terms of k-eff results. When compared to criticality benchmarks, reactor physics experiments prove more challenging due to the multitude of isotopes, reactions, and the influence of geometry. Nevertheless, these experiments accurately represent real-world conditions, being for example more sensitive to the angular distributions of the scattering cross sections, highlighting aspects than can be overlooked in criticality benchmarks, so they are highly valuable for testing evaluations for present or future reactors in operation. Shielding and transmission experiments offered additional insights beyond the neutron energy of criticality and reactor benchmarks.

Regarding the use of measurements in Light Water Reactors for nuclear data validation, some general conclusions can also be drawn:

- They fall into the category of integral benchmarks with low fidelity for nuclear data adjustment. The use of these experimental data may provoke many compensating effects due to various multi-physics phenomena involved and many different sources of uncertainties. Definitely, PWR experimental data are not clean benchmarks.
- They can be utilized to assess the performance of a nuclear data library in a specific neutron environment (thermal neutrons in LWRs at different burnup/irradiation steps).
- They serve to identify general trends due to nuclear data. Consistent trends, comparable to reactor-level trends, can also be observed at both pin-cell level and fuel-assembly levels. Moreover, uncertainty quantification (due to nuclear data uncertainties) can also be conducted

at this level. This information can be useful for a deeper understanding of safety and design margins.

- It is worth mentioning that Light Water Reactor measurements are proprietary, which is an added difficulty of these data to be use for nuclear data validation.

Finally, other applications that were not addressed in this study but are gaining significance were identified. Validation and benchmarking of JEFF evaluations before a final release of a library should also be performed for such applications.

5. References

[Becares, 2024] V. Bécares, Validation of fission product nuclear data against MINERVE-CERES pile oscillation experiments. CIEMAT report DFN/IN-04/II-24 (July 2024).

[Cabellos, 2022] O. Cabellos et al., Benchmarking and Validation with JEFF-4T2.23, JEFDOC 2239 , JEFF Nuclear Data Week, April 25-28, 2022.

[Cabellos, 2023] O. Cabellos, Feedbacks on Processing and Benchmarking of JEFF4-T3, JEFDOC 2303 , JEFF Nuclear Data Week, November 27 30, 2023.

[Capote, 2024] R. Capote et al, Update of INDEN evaluations: Validation and challenges, JEFDOC2334, JEFF Nuclear Data Week, April 2024.

[García-Herranz, 2024] N. García-Herranz, O. Cabellos, A. Jiménez-Carrascosa, D. Bernard, I. Kodeli, G. Zerovnik, S. van der Marck, Report on reactor and shielding C/E validation and nuclear data trends, SANDA Project, Deliverable D5.7, June 2024.

[Leclaire, 2022] N. Leclaire and S. van der Marck, Report on critical benchmark C/E validation and nuclear data trends, SANDA Project, Deliverable D5.8, February 2022.

[Plompen, 2020] A. Plompen et al., The joint evaluated fission and fusion nuclear data library, JEFF-3.3, Eur. Phys. J. A., pp. 1-107 (2020).

[Radulescu, 2012]. G. Radulescu, J.Wagner, Burn-up CreditCriticality safetyBenchmark Phase VII—UO2 fuel: study of spent fuel compositions for long-term disposal, Tech. Rep. OECD/NEA-6998,Working Party on Nuclear Criticality Safety (2012).

6. Acknowledgements

The ICSBEP, IRPHEP and SINBAD databases have been obtained through the Computer Programs Services of OECD/NEA Nuclear Data Bank; MCNP code through the Radiation Safety Information Computational Center (RSICC) of Oak Ridge National Laboratory (ORNL, USA), and SCALE6.3beta through Oak Ridge National Laboratory. Part of the work related to MINERVE/CERES experiments has also been partially supported by the ENRESA-CIEMAT agreement “*Tecnologías Disponibles para la Transmutación de Radionucleidos de Vida Larga*”.

7. Derived publications

The following publications were derived from work related to the SANDA Task 5.2 “Validation studies using existing experiments” reported in this deliverable.

7.1. International conferences

- [1] [Jiménez-Carrascosa, ND2022] Antonio Jiménez-Carrascosa, Oscar Cabellos, Carlos Javier Díez, and Nuria García-Herranz, Processing of JEFF nuclear data libraries for the SCALE Code System and testing with criticality benchmark experiments, ND2022, EPJ Web of Conferences 284, 14009 (2023), <https://doi.org/10.1051/epjconf/202328414009>

7.2. Workshops

- [2] [JEFDOC-1991] O. Cabellos, “Feedbacks on JEFF-3.3 Evaluation: Uncertainty in keff for some ICSBEP Outliers, PWR Critical Boron Letdown Curve and Additional integral data testing using reaction rates in critical assemblies”, JEFF Meeting, April 2020. JEFDOC-1991 (video-conference).
- [3] [JEFDOC-2015] O. Cabellos, M. García-Hormigos, B. Moreno and S. Sánchez-Fernández, “The importance of using different integral benchmarks to provide valuable feedbacks to the evaluation process” JEFF Meeting and JEFF-CG, Nov 2020. JEFDOC-2015 (video-conference).
- [4] [JEFDOC-2041] O. Cabellos, Overview of Processing, Verification and Benchmarking activities at UPM, JEFF Nuclear Data Week, April 28, 2021, JEFDOC-2041 (video -conference).
- [5] [JEFDOC-2091] O. Cabellos, A. Jiménez-Carrascosa, N. García-Herranz, G. de Alcázar, Overview of Processing, Testing of the JEFF-3.3 with IRPhEP/LWR KRITZ Benchmarks, JEFF Nuclear Data Week, November 22-26, 2021, JEFDOC-2091 (in-person).
- [6] [JEFDOC-2097] A. Jiménez-Carrascosa, O. Cabellos, N. García-Herranz, F. Chafer. Impact of Doppler calculation in SEFOR benchmark due to the differences between JEFF-3.3 and JEFF-3.1.1. JEFF Nuclear Data Week, November 22-26, 2021, JEFDOC-2097.
- [7] [JEFDOC-2107] A. Jiménez-Carrascosa, O. Cabellos, C.J. Díez, N. García-Herranz Overview of Processing of JEFF nuclear data libraries for the SCALE Code System, JEFF Nuclear Data Week, November 22-26, 2021 (in-person).
- [8] [JEFDOC-2239] M. Astigarraga, O. Cabellos, Benchmarking and Validation with JEFF-4T2.2, JEFF Nuclear Data Week, April 25-28, 2022, JEFDOC-2239 (in-person).
- [9] [JEFDOC-2303] O. Cabellos, Feedback on Processing and Benchmarking of JEFF-4T3, JEFF Nuclear Data Week, November 27-30, 2023, JEFDOC-2303 (in-person).
- [10][JEFDOC-2316] O. Cabellos, Feedbacks on Processing and Benchmarking for JEFF4-T3, JEFF Nuclear Data Week, April 2024, JEFDOC-2316.
- [11][CSEWG, 2023] O. Cabellos, Feedback on ENDF/B-VIII.1b2 on a selection of Benchmarks, CSEWG Meeting, November, 2023 (video -conference).
- [12][IAEA/INDEN-Nov 2020] O. Cabellos, “Indications from integral benchmarks on U-235, U-238 and Pu-239 evaluations” IAEA CM of the INDEN on Actinide Evaluation in the Resonance Region, 17-19 Nov 2020 (video-conference).
- [13]N. Leclaire, *Calculation of Integral experiments with the MORET 5 code in support of the JEFF-4.0T2 nuclear data validation*, JEFF meeting, November 2022, JEFDOC-2172
- [14]N. Leclaire, *Feedback on JEFF-4T1 on a selection of critical experiments*, JEFF meeting, April 2022, JEFDOC-2140
- [15]N. Leclaire, *Calculation of the kritz-LWR-RESR-004 benchmark with MORET 5 CODE*, JEFF meeting, November 2021, JEFDOC-2090
- [16]J.D. Bartos, *First benchmarking results for JEFF-4t3*, JEFF meeting, April 2024, JEDOC-2350

- [17]S.C. van der Marck, *The Duke IRPhE benchmark for depletion reactivity*, JEFF meeting, November 2023, JEFDOC-2286
- [18]S.C. van der Marck, *Benchmark results for JEFF-4t2*, JEFF meeting, April 2023, JEFDOC-2230
- [19]S.C. van der Marck, *Temperature dependence of reactivity: CREOLE and KRITZ benchmarks*, JEFF meeting, November 2022, JEFDOC-2173
- [20]S.C. van der Marck, *First results of criticality safety benchmark calculations using JEFF-4T1*, JEFF meeting, November 2022, JEFDOC-2143
- [21]S.C. van der Marck, *Observations based on benchmarking results for JEFF-4T0*, JEFF meeting, April 2021, JEFDOC-2094

7.3. Doctoral thesis

- [22][Jiménez-Carrascosa, Thesis] Antonio Jiménez-Carrascosa “Methodologies for enhancing the Neutronic Assessment of Sodium-Cooled Fast Reactors: From Nuclear Data to transient Analysis”, Thesis Doctoral, UPM, February 2023

7.4. Dissemination and Education

- [23][Cabellos, ARIEL-2022] O. Cabellos, “Reference integral experiments databases and validation of nuclear data”, ARIEL-H2020 - International on-line school on nuclear data: NuDataPath – February 21st to March 4th, 2022, <https://agenda.ciemat.es/event/3201/>
- [24][Cabellos, SCALE 202] Oscar Cabellos, Nuria García-Herranz and Antonio Jiménez-Carrascosa, “UPM activities in the framework of SANDA project using SCALE system”, 6th Annual SCALE Users' Group Workshop, April 28, 2022, <https://www.ornl.gov/file/01oscarcabellosupm/display>
- [25][García-Herranz, 2022] N. García-Herranz, A. Jiménez-Carrascosa, O. Cabellos. UPM activities under EC project SANDA in line with SFR-UAM. OECD/NEA SFR-UAM meeting, Aix-en-Provence, France, June 2-3 2022.

8. Appendix 1: Validation of fission product data against MINERVE-CERES pile oscillation experiments

8.1. Introduction

Task 5.2 of the SANDA project is dedicated to validation studies of nuclear data using existing integral experiments. While differential experiments typically involve measuring the value of the cross section of a given isotope at a given energy of the incident neutrons, integral experiments try to infer the value of these cross sections from the measurement of global parameters of nuclear systems. These can be, for instance, the criticality constant of a nuclear reactor or the neutron flux distribution in a given medium.

Although integral experiments do not provide detailed information about the energy dependence of the nuclear cross sections, they have at least two major advantages over differential experiments. First, their analysis is usually more straightforward than in the case of differential measurements. This was especially relevant in the past, when computational capabilities were much less developed than today. Second, they can provide data measured in environments more representative of practical applications. This is particularly relevant since even the most advanced neutron transport codes coupled with the most recent versions of general-purpose nuclear data libraries fail to meet the required target accuracies for many parameters of advanced nuclear systems, as shown, for instance, by uncertainty studies performed under task 5.1 of the SANDA project [Panizo 2024].

For this reason, integral experiments have been included under task 5.3 of the SANDA project. In particular, SANDA subtask 5.3.1 is devoted to performing neutron transmission experiments with the same samples measured by the pile oscillation technique at the MINERVE reactor during the CERES program [Dean 2007]. The CERES program was devoted to study the fission products (FPs) and therefore a set of samples of UO₂ containing some relevant FPs were measured.

The analysis of pile oscillation experiments with Monte Carlo codes is cumbersome, since it requires calculating small differences between large numbers that are usually masked by the stochastic uncertainties of the method. In the framework of task 12.1 of the previous EU FP7 CHANDA project [Leconte 2017], and with the aim of analyzing integral measurements of the capture cross section of ²⁴¹Am performed at the MINERVE reactor (AMSTRAMGRAM project), a calculation benchmark was carried out to evaluate and cross-compare techniques to calculate small reactivity differences. However, major discrepancies in the results among codes were found, including significant differences between the perturbative tools available in MCNP (PERT and KPERT). Therefore, alternative calculation schemes were proposed. For this reason, in task T5.2 of the SANDA Project, CIEMAT proposed applying these calculation schemes to the analysis of a set of MINERVE/CERES pile oscillation experiments which are available in the IRPhE database [Santamarina 2014, Santamarina 2016]. This analysis was particularly useful given that transmission measurements with the same samples measured in the MINERVE/CERES program were envisaged under task 5.3.1 of the SANDA project [Noguere 2023].

Overall, this section is structured in three major blocks. First, the model of the MINERVE reactor in the configuration used during the CERES experiments is presented in sub-section 8.2. Then, the calculation schemes applied to analyse the pile oscillation experiments are described in sub-section 8.3. The results are presented in sub-section 8.4. The calculations presented in this work have all been performed with the MCNP6.2 code [Werner 2017].

8.2. MCNP modelling of the CERES experiments at MINERVE

The MINERVE reactor [Fougeras 2005, Bignan 2010] was a zero-power, pool-type, light-water moderated research reactor that was in operation at CEA-Cadarache between 1977 and 2017. It was mainly used for integral cross section measurements through the pile-oscillation technique.

The MINERVE reactor (Figure 3) was made up of a core consisting of an array of 3% enriched UO_2 fuel rods surrounded by aluminium and graphite reflector blocks, all placed within a light-water pool. Some extra fuel, in the form of highly-enriched uranium plate fuel elements, was placed at the core periphery, within the graphite reflector blocks. Although it was a light-water moderated reactor, the spectra in the core centre (where the oscillation experiments were performed) could be adjusted by adding or removing fuel rods around it.

In pile oscillation experiments, a (small) sample was introduced at the centre of the reactor in a critical state, so that it becomes (slightly) subcritical or supercritical as a result of this introduction. To keep the reactor in a critical state, the position of a pilot control rod was adjusted so that the count rate in a pilot detector remains constant. In fact, to facilitate the analysis of the measurements, reference samples with a similar geometry than the samples being studied were also measured. In this way, the reactivity impacts of other components of the oscillator are cancelled and the impact of the measured samples in the reactivity can be isolated.

If this pilot rod is correctly calibrated, the impact in the reactivity of the sample can be quantified. MINERVE's pilot rod provided the reactivity in a particular unit called kUP, the equivalence provided in [Santamarina 2014] is $100 \text{ kUP} = 1.4 \text{ pcm}$. However, it is worth remarking that the relative impacts of the samples can be measured even without an accurate calibration of the pilot rod.

In the CERES program, two sets of samples were measured. The first one consisted of ten samples of sintered UO_2 containing different amounts of fission products of interest (natural Sm, Sm-147, Sm-149, Sm-152, natural Nd, Nd-153, Nd-155, Gd-155, Eu-153 and Rh-103); the reference sample was a sample of sintered UO_2 without fission products. The second set was a set of three samples of compacted UO_2 containing Cs-133, Mo-99 and Tc-99, respectively; in this case, the reference sample was a sample of compacted UO_2 without fission products. All samples were in the shape cylinders of about 1 cm diameter and 10 cm length and were placed within a Zircalloy-4 container. The oscillator rod both above and below them was filled with 3% enriched UO_2 pellets, similar to the other fuel rods in the reactor core. A detail of the samples as modelled in MCNP is presented in Figure 4.

A detailed MCNP model of the MINERVE reactor, developed for the OSMOSE project, is publicly available [Perret 2004]. This model, together with the information about the samples provided in the IRPhE documentation has been used to develop the MCNP model used in this work. As reference nuclear data library we have considered the ENDF/B-VII.1 [Chadwick 2011] library as distributed with the MCNP code itself, and all results presented in this work have been calculated with this library, unless stated otherwise.

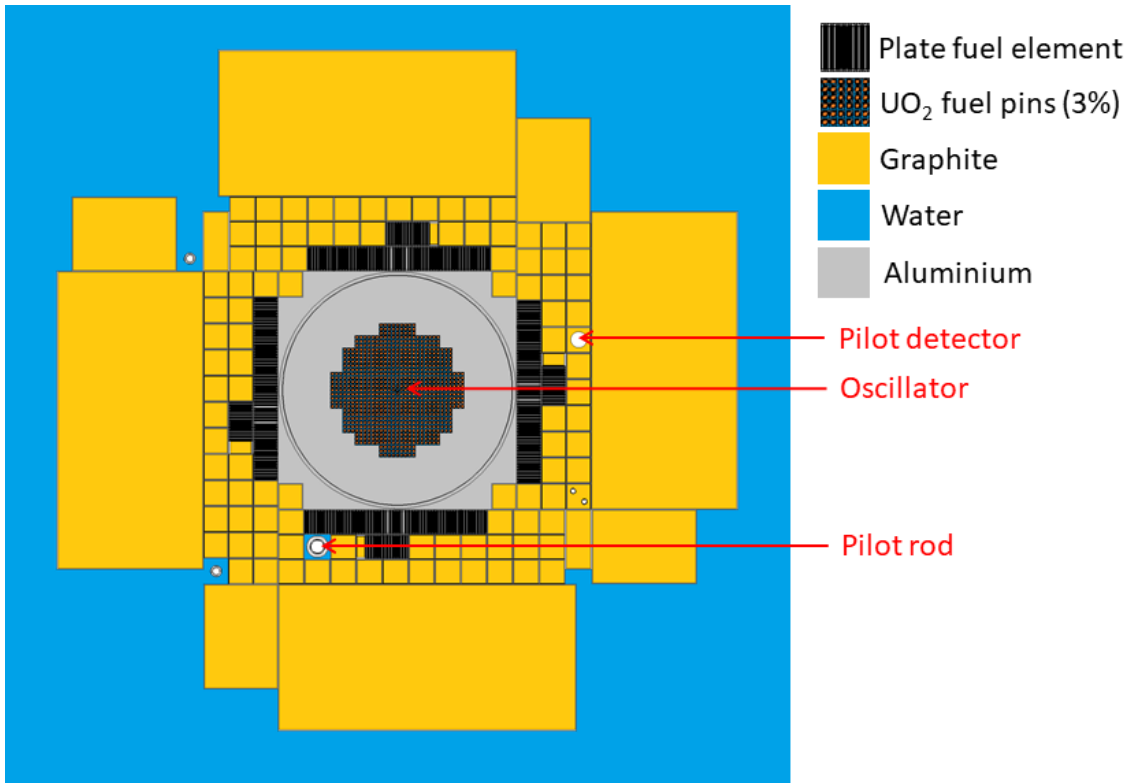


Figure 3. Schematics of the MINERVE reactor in the CERES configuration.

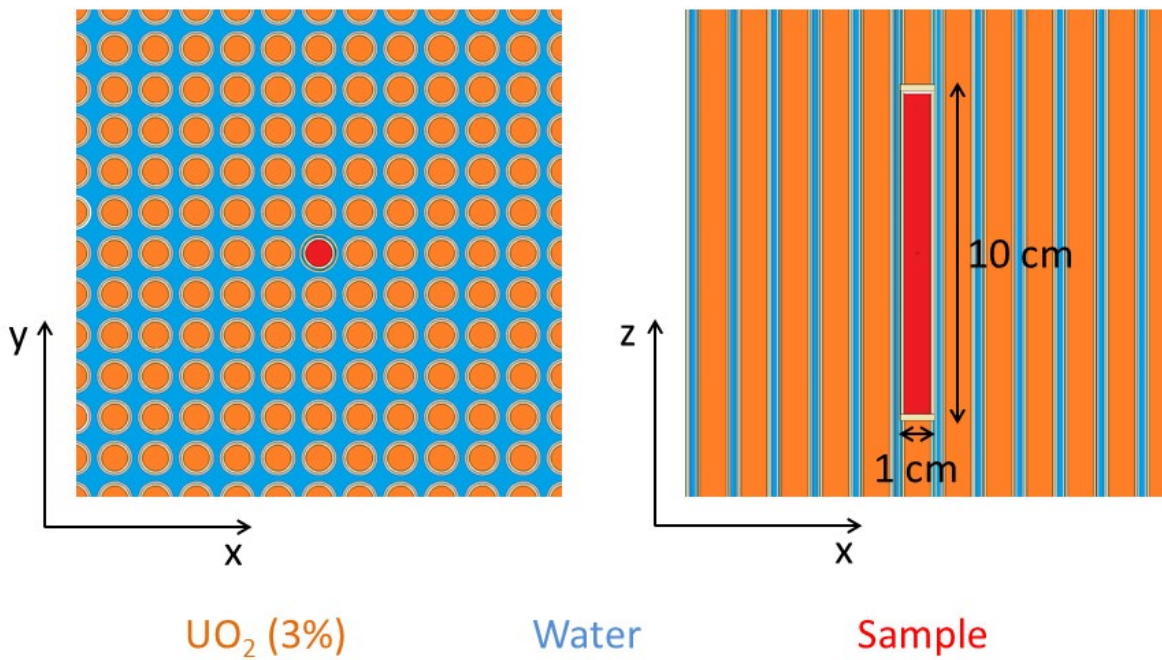


Figure 4. Detail of the oscillation sample.

8.3. Calculations

Overall, in this work three techniques have been used to calculate the small reactivity differences due to the introduction of the oscillation samples in the MINERVE core: a variant of the EigenValue Difference Method (EVDM), an adjoint-weighted perturbation calculation (with calculated adjoint fluxes and reaction rates) and MCNP KPERT card (which also makes use of adjoint-weighted perturbation calculation). An illustration of the neutron spectra found in MINERVE/CERES is shown in Figure 5.

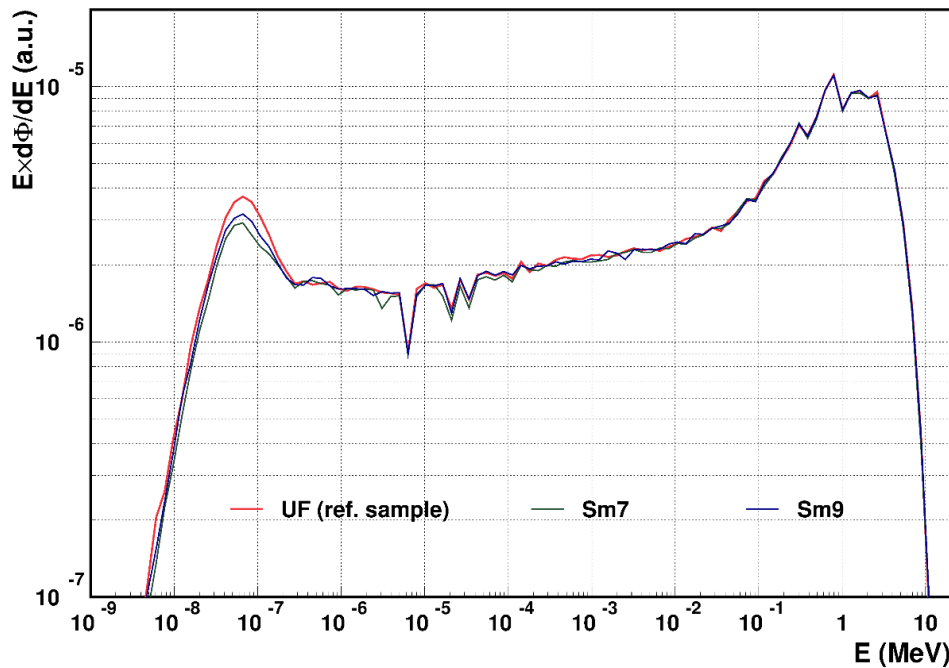


Figure 5. Neutron spectra in MINERVE/CERES sample position with the reference UO_2 sample (UF) and a samples containing ^{147}Sm (Sm7) and ^{149}Sm (Sm9).

8.3.1. Eigenvalue Difference Method (EVDM)

This technique simply consists in performing two eigenvalue calculations, one with the sample being measured and another one with the reference sample. This is the most straightforward method and the one making the less assumptions or approximations. On the other hand, it has the disadvantage that, when the reactivity difference between the samples is small, Monte Carlo codes cannot do this calculation with enough precision, as it would require an unacceptably large number of histories to get statistical errors smaller than the reactivity difference being calculated.

For this reason, in this work the EVDM technique has not been implemented directly but we have instead made the calculations with an increased sample density to reduce the relative statistical error of the calculation by having a larger reactivity difference. Some more details about the implementation are provided in Figure 6. The disadvantage of this approach is that as sample density increases, so does the self-shielding effect, which prevents a simple linear interpolation to determine the reactivity effect of the sample at its nominal density. For this reason, we have considered several density values ($\times 4$, $\times 5$, $\times 7$ and $\times 10$) and performed a fit to a second order polynomial ($f(x) = ax + bx^2$). The adjustments have been calculated with CERN's MINUIT software [James 1994] supplied with the PAW package [CERN 1995]. Notice that the parameter a corresponds to the impact of the sample in the reactivity in the absence of self-shielding effects, while b represents the correction introduced by these effects.

The values of k_{eff} obtained with MCNP for the different samples, as well as the results of this second order fit, are shown in Figure 7 to Figure 10. The numerical values are listed in Table 8 and Table 9. For the Sm7 sample a different range of densities has been considered ($\times 2$ to $\times 5$); the reason is that this sample has a larger impact in the reactivity (about twice) than the other samples, and hence the non-linear effects start to be relevant at lower values of the density increase.

In any case, it can be observed in the figures that with this range of densities non-linear effects are very apparent, which makes of little use considering further increases of the density. On the other hand, it can be observed in Table 8 and Table 9 that the χ^2 values of the fit tend to be rather low (< 1). This indicates a very good adjustment to the model, but it must be also taken into account that the uncertainty in the reactivity differences is still relatively high, in spite of the increase of the density of the samples and to the large statistics used to calculate the values of k_{eff} (1-2 pcm³). It is likely possible to optimize the number of points and the density ranges to reduce biases and increase the precision, but this will require a large amount of work (in particular, for performing an analysis on a sample-by-sample basis) that is beyond the scope of this study.

Anyway, this calculation scheme is advantageous in computational terms with respect to the conventional EVDM method. From the values listed in Table 8, it is possible to reach a precision of 0.44 pcm in the value of a (which, as stated above, it is the reactivity impact of the sample in the absence of self-shielding effects) with a total of three calculations with 1 pcm precision (reference sample and the measured sample at $\times 4$ and $\times 5$ its nominal density) and other two calculations (density $\times 7$ and $\times 10$) with 2 pcm precision (20% the number of neutron histories). As detailed in , achieving the same precision with the traditional EVDM would require two calculations with 0.31 pcm precision, or about ten times the number of neutron histories, which results is 6 times more statistics overall. It can be observed in Table 8 that increasing the number of calculations for some samples (Sm9, Sm2, Nd3 and Gd5 for ENDF/B-VII.1 and Sm9, Sm2, Nd3, Nd5 and Rh) does not result in a significant improvement in the precision. Still, the computational time required is very large and the calculations have been only performed with two nuclear data libraries (ENDF/B-VII.1 and JEFF-3.3). In any case, given the small differences between libraries (as evidenced by the calculations performed with the adjoint-weighted perturbation theory, see in next section) the precision required to observe meaningful differences between nuclear data libraries would be prohibitive.

As a final comment, the calculations with different samples and at different densities have been performed with different random number sequences. As the cases simulated are very similar, this is the way to prevent correlations in the results due to different calculations sharing a large number of neutron stories.

³ part per cent mille (per hundred thousand).

EVDM implemented in this work

Reference sample	Density ×4	Density ×5	Density ×7	Density ×10	Total no. histories
6.25×10 ⁹ hist. (1 pcm)	6.25×10 ⁹ hist. (1 pcm)	6.25×10 ⁹ hist. (1 pcm)	1.25×10 ⁹ hist. (2 pcm)	1.25×10 ⁹ hist. (2 pcm)	2.125×10 ¹⁰ hist. for 0.44 pcm

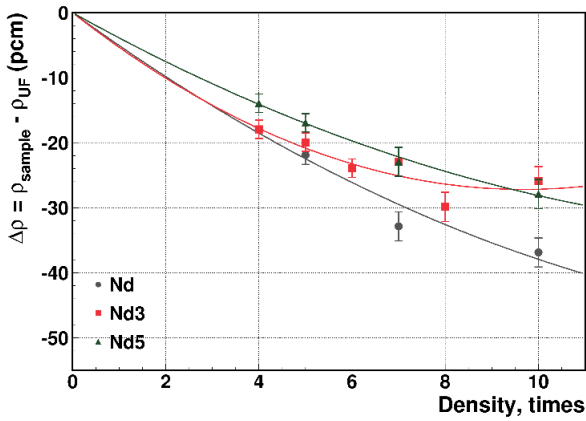
“Conventional” EVDM

Reference sample	Measured sample (nominal dens.)				Total no. histories
0.31 pcm → ×10 statistics → 6.25×10 ¹⁰ hist.	0.31 pcm → ×10 statistics → 6.25×10 ¹⁰ hist.				12.5×10 ¹⁰ for 0.44 pcm

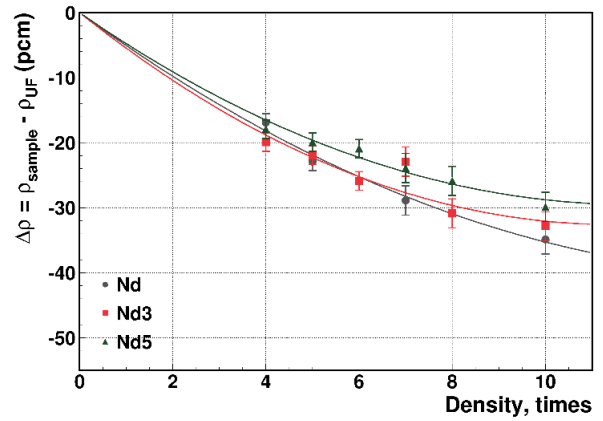
×6 (3-9) reduction in computer time



Figure 6. Gain in computer time with the variant of the EVDM method implemented in this work.

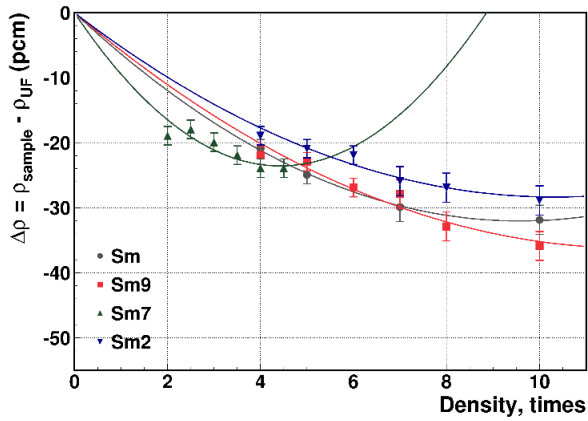


(a) ENDF/B-VII.1

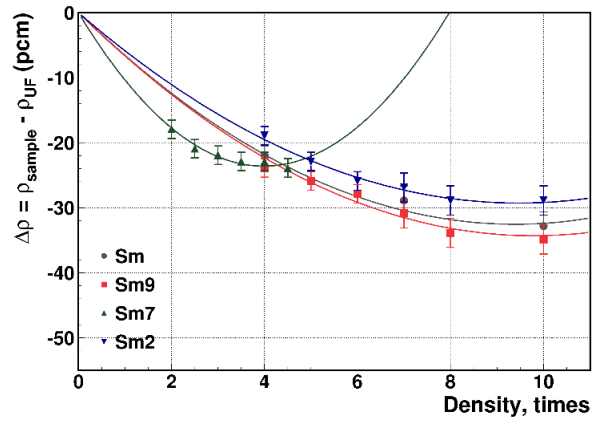


(b) JEFF-3.3

Figure 7. Δρ vs. density for Nd (nat), Nd143 and Nd145 samples.

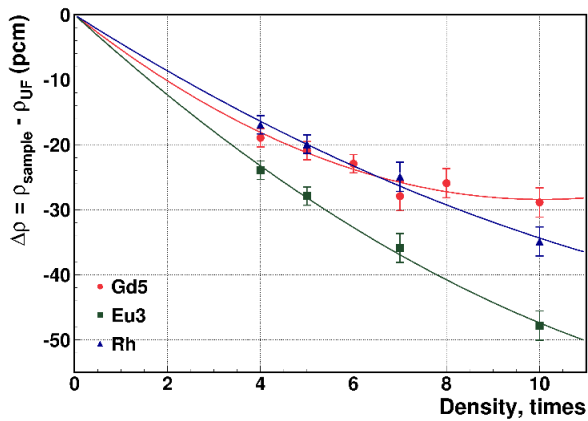


(a) ENDF/B-VII.1

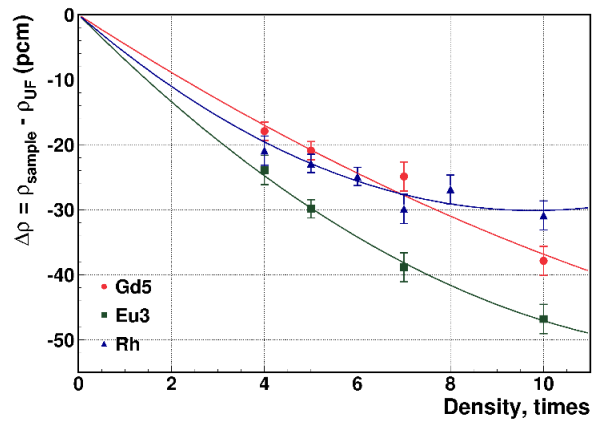


(b) JEFF-3.3

Figure 8. $\Delta\rho$ vs. density for Sm (nat), Sm149, Sm147 and Sm152 samples. Notice the different range of density increases for the case of Sm-147.

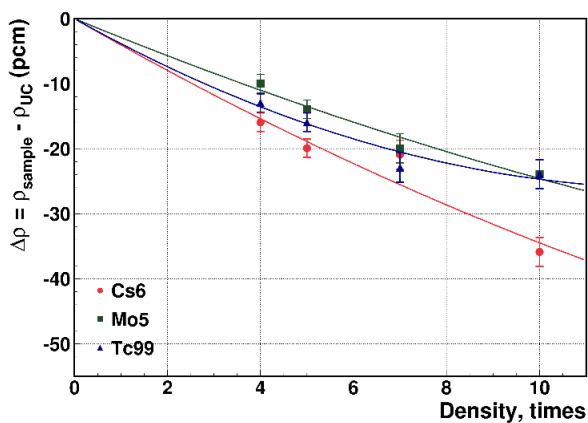


(a) ENDF/B-VII.1

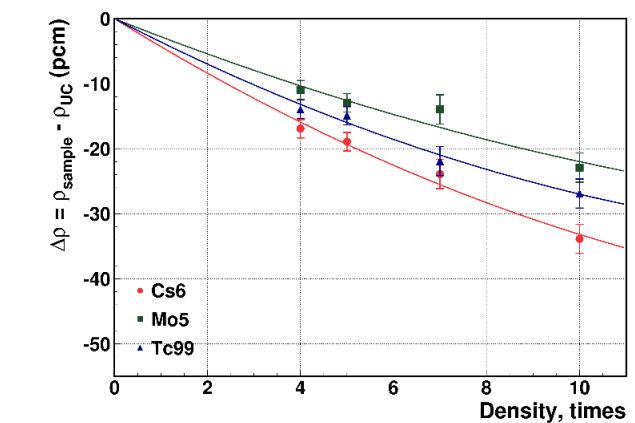


(b) JEFF-3.3

Figure 9. $\Delta\rho$ vs. density for Gd155, Eu153 and Rh103 samples.



(a) ENDF/B-VII.1



(b) JEFF-3.3

Figure 10. $\Delta\rho$ vs. density for Cs133, Mo95 and Tc99 samples.

Table 8. Values of the k_{eff} of the MINERVE reactor with the oscillation sample density multiplied by several factors. For compactness, the values listed are $k_{eff} - 1$, in pcm units, i.e. 238 corresponds to $k_{eff}=1.00238$. The results of the fit of the reactivity differences ($\Delta\rho = \frac{k_{eff,sample}-1}{k_{eff,sample}} - \frac{k_{eff,ref}-1}{k_{eff,ref}}$) vs. the density multiplication factor to a function of the shape $f(x) = ax + bx^2$ are also listed.

Dens.	UF (reference)									UC (reference)		
	200 ± 1									202 ± 1		
	Sm	Sm9	Sm2	Nd	Nd3	Nd5	Gd5	Eu3	Rh	Cs6	Mo5	Tc99
×4	179 ± 1	178 ± 1	181 ± 1	182 ± 1	182 ± 1	186 ± 1	181 ± 1	175 ± 2	185 ± 2	186 ± 1	192 ± 1	189 ± 1
×5	175 ± 1	177 ± 1	179 ± 1	178 ± 1	180 ± 1	183 ± 1	179 ± 1	172 ± 1	180 ± 1	182 ± 1	188 ± 1	186 ± 1
×6	---	173 ± 1	178 ± 1	---	176 ± 1	---	177 ± 1	---	---	---	---	---
×7	170 ± 2	172 ± 2	174 ± 2	167 ± 2	177 ± 2	177 ± 2	172 ± 2	164 ± 2	175 ± 1	181 ± 2	182 ± 2	179 ± 2
×8	---	167 ± 2	173 ± 2	---	170 ± 2	---	174 ± 2	---	---	---	---	---
×10	168 ± 2	164 ± 2	171 ± 2	163 ± 2	174 ± 2	172 ± 2	171 ± 2	152 ± 2	165 ± 2	166 ± 2	178 ± 2	178 ± 2
Least squares fit to $f(x) = ax + bx^2$												
a	-6.69 ±0.44	-6.03 ±0.40	-5.49 ±0.40	-5.19 ±0.44	-5.62 ±0.40	-4.00 ±0.40	-5.65 ±0.41	-6.53 ±0.44	-4.54 ±0.44	-4.11 ±0.44	-2.95 ±0.44	-4.00 ±0.44
b	0.35 ±0.06	0.25 ±0.06	0.27 ±0.05	0.14 ±0.06	0.29 ±0.05	0.12 ±0.06	0.28 ±0.06	0.18 ±0.06	0.11 ±0.06	0.07 ±0.06	0.05 ±0.06	0.15 ±0.06
χ^2	0.03	0.78	0.48	1.42	1.09	0.07	0.52	0.26	0.31	2.65	0.65	0.74

(a) ENDF/B-VII.1

Dens.	UF (reference)									UC (reference)		
	238 ± 1									238 ± 1		
	Sm	Sm9	Sm2	Nd	Nd3	Nd5	Gd5	Eu3	Rh	Cs6	Mo5	Tc99
×4	216 ± 1	214 ± 1	219 ± 1	221 ± 1	218 ± 1	220 ± 1	220 ± 2	214 ± 2	217 ± 2	221 ± 1	227 ± 1	224 ± 1
×5	212 ± 1	212 ± 1	215 ± 1	215 ± 1	216 ± 1	218 ± 1	217 ± 1	208 ± 1	215 ± 1	219 ± 1	225 ± 1	223 ± 1
×6	---	210 ± 1	212 ± 1	---	212 ± 1	217 ± 1	---	---	213 ± 1	---	---	---
×7	209 ± 2	207 ± 2	211 ± 2	209 ± 2	215 ± 2	214 ± 2	213 ± 2	199 ± 2	208 ± 2	214 ± 2	224 ± 2	216 ± 2
×8	---	204 ± 2	209 ± 2	---	207 ± 2	212 ± 2	---	---	211 ± 2	---	---	---
×10	205 ± 2	203 ± 2	209 ± 2	203 ± 2	205 ± 2	208 ± 2	200 ± 2	191 ± 2	207 ± 2	204 ± 2	215 ± 2	211 ± 2
Least squares fit to $f(x) = ax + bx^2$												
a	-6.93 ±0.44	-7.01 ±0.40	-6.19 ±0.40	-5.23 ±0.44	-5.70 ±0.40	-4.97 ±0.40	-4.63 ±0.44	-7.19 ±0.51	-6.15 ±0.45	-4.42 ±0.44	-2.84 ±0.44	-3.69 ±0.44
b	0.37 ±0.06	0.36 ±0.05	0.33 ±0.06	0.17 ±0.06	0.25 ±0.05	0.21 ±0.06	0.10 ±0.06	0.25 ±0.06	0.31 ±0.06	0.11 ±0.06	0.06 ±0.06	0.10 ±0.06
χ^2	0.32	0.59	0.10	0.71	1.48	0.58	1.15	0.14	0.67	0.62	0.99	0.51

(b) JEFF-3.3

Table 9. Values of the k_{eff} of the MINERVE reactor with the Sm7 sample density multiplied by several factors, for the ENDF/B-VII.1 and the JEFF-3.3 libraries. Same comments than in Table 8.

Dens.	ENDF/B-VII.1	JEFF-3.3
UF (ref.)	200 ± 1	238 ± 1
×2	181 ± 1	220 ± 1
×2.5	182 ± 1	217 ± 1
×3	180 ± 1	216 ± 1
×3.5	178 ± 1	215 ± 1
×4	176 ± 1	215 ± 1
×4.5	176 ± 1	214 ± 1
×5	175 ± 1	211 ± 1
Least squares fit it to $ax + bx^2$		
a	-11.64 ±0.84	-11.84 ±0.84
b	1.20 ±0.22	1.49 ±0.22
χ^2	1.20	0.19

8.3.2. Perturbation theory

This is the traditional calculation scheme to analyze pile oscillation experiments. Under this theory, the impact in the reactivity of a small change in the system is calculated as:

$$\Delta\rho = \frac{\langle \Phi_0^\dagger | \lambda_0 \Delta\hat{F} - \Delta\hat{M} | \Phi \rangle}{\langle \Phi_0^\dagger | \hat{F}_0 | \Phi \rangle} \quad (\text{Eq. 3.1})$$

where Φ represents the neutron flux in the perturbed state, Φ_0^\dagger is the adjoint flux in the reference state, \hat{F}_0 is the neutron creation (fission) operator in the reference state, $\lambda_0 = 1/k_{eff,0}$ (i.e. the inverse of the criticality constant in the reference state) and $\Delta\hat{F}$ and $\Delta\hat{M}$ represent, respectively, the perturbation introduced in the neutron creation and migration/losses (transport) operators. The brackets denote integration over all variables of the phase space (position and neutron velocity).

For the pile oscillation experiments analyzed in this work, the perturbation is simply due to the introduction of a neutron absorber, so $\Delta\hat{F} = 0$ and $\Delta\hat{M} = \sigma_{abs}(E)$ in the volume of the sample and zero outside it. Furthermore, if we are just interested in calculating the relative effects in the reactivity of the different samples, the denominator in Eq. 3.1 will be the same for all samples and we can limit ourselves to calculate the numerator of Eq. 3.1. Hence, the quantity that has been calculated with MCNP is:

$$\langle \Phi_0^\dagger | \Delta\hat{M} | \Phi \rangle = \int_{\vec{r}=\text{sample}} \int_E \Phi_0^\dagger(E) \sigma_{abs}(E) \Phi(E) d\vec{r} dE \simeq \sum_i \Phi_{0,i}^\dagger \sigma_{abs,i} \Phi_i \Delta E_i \quad (\text{Eq. 3.2})$$

where $\sigma_{abs,i} \Phi_i \Delta E_i$ has been calculated with an MCNP flux tally (F4) in the sample cell using a tally multiplier tally (FM card) to multiply it by neutron capture cross section. As stated above, the integral on the space (\vec{r}) extends only over the volume of the sample. Note that if the tally results are retrieved with the NONORM option, the values obtained will already take into account the factor ΔE_i . The adjoint flux $\Phi_{0,i}^\dagger$, for its part, cannot be obtained in a straightforward manner with MCNP. In Annex 1, it is described the procedure used in this work to calculate it with MCNP. As a final comment, the energy structure used for these calculations is the SHEM energy mesh [Santamarina 2007, Santamarina 2016].

Overall, the main advantage of this perturbative technique is that it is much less computer intensive than the EVDM method discussed above. The disadvantages are that simplifying hypotheses are made (the perturbation introduced by the samples is limited to the absorption). Furthermore, as stated above, it requires the calculation of the adjoint flux, which is cumbersome with Monte Carlo codes.

8.3.3. MCNP KPERT card

MCNP6.2 also implements a functionality to calculate perturbations in k_{eff} using the adjoint-weighted perturbation theory described in the previous section: the KPERT card. Although this offers a straightforward way to perform the perturbative calculations described above without the need to calculate the adjoint flux, work performed during Task 12.1 of CHANDA showed that KPERT does not always provide accurate results. This was, as stated above, the main reason that drove the development of the modified EVDM method described above.

Anyway, we also have calculated the reactivity effect with this card, in order to compare with the results obtained with the EVDM method and the perturbation theory (with a separate calculation of the adjoint flux). For this, we have started from the reference source and have had its composition and densities replaced by the composition and densities of the individual samples.

8.4. Calculation results and discussion

The main findings of the reactivity performed with all these three techniques are presented in this section.

- 1) The results of the reactivity differences due to the introduction of the samples calculated with the modified EVDM method are presented in Figure 11 and Table 10, for the ENDF/B-VII.1 library, and Figure 12 and Table 11, for the JEFF-3.3 library. The absolute reactivity differences obtained with this method are listed, as well as the differences adjusted to the experimental data by a least-squares fit. This fit was performed excluding Sm-147, because of its large difference in the reactivity with respect to the other samples. The experimental values represented in the figure use the calibration provided in IRPhE's documentation⁴ [Santamarina 2016].

When these calculated results are compared with the experimental ones considering the values of the calibration provided in IRPhE's documentation, it is observed a general trend of underestimating the reactivity differences. However, when the relative results after performing a least-squares fit to the experimental results are considered (to take into account only relative differences between samples), a very good agreement between experiments and calculations is observed. Both for the ENDF/B-VII.1 and JEFF-3.3 libraries, out of 13 samples, the C/E (calculation/experiment) ratios are within 1- σ for 9 of them and between 1- σ and 2- σ for the remaining. C/E ratios are within about $\pm 10\%$ in all the cases, with an uncertainty (mostly due to the statistical uncertainty in the calculations) also about 10%. For the samples with the lower reactivity effect (Mo5, Tc99), C/E ratios can reach up to about $\pm 20\%$, but the uncertainty also increases to about 20%.

⁴ MINERVE's pilot control provides reactivity results in units called kUP, which have to be calibrated to obtain the value in pcm. The value provided in [Santamarina 2016] is 100 kUP = 1.4 pcm, although this equivalence is stated to be approximate. In any case, for comparing the relative references between the samples the value of this equivalence is not relevant.

- 2) Regarding the results obtained with the perturbation theory (Figure 13 and Table 12), in this case only relative results are provided, obtained by performing a least-squares fit of the calculated and the experimental results, again excluding Sm-147. Since the results obtained with perturbation theory have much less statistical uncertainty than the results obtained with the EVDM method, calculation and experimental results are not in agreement within experimental errors. However, perturbation theory calculations also yield C/E ratios within about $\pm 10\%$ (up to 16%) for all samples. The poorest agreement was for Sm-147, with a C/E ratio of 0.75 (take into account that this sample was excluded from the fit, as stated above).

Furthermore, the higher computational efficiency of perturbation theory has allowed to perform the calculations with different nuclear data libraries, namely ENDF/B-VIII.0 [Brown 2018], JENDL-5 [Iwamoto 2023], JEFF-3.3 [Plompen 2020] and three beta releases (T1, T2 and T3) of the upcoming JEFF-4.0. In order to isolate the effect of the isotope being measured, only the cross sections of these isotopes have been changed, all other materials and isotopes have retained cross sections from the ENDF/B-VII.1 library used as reference. In any case, no significant difference between nuclear data libraries has been found.

- 3) Finally, regarding the results obtained with the KPERT card (Figure 14 and Table 13), it can be observed that the absolute reactivity differences obtained with this technique tend to overestimate the experimental reactivity measurements. This is contrary to the results obtained with the EVDM method. When relative results are considered (through a least-squares fit of the calculated results to the experimental ones, again excluding Sm-147) a somewhat larger dispersion (with respect to the EVDM and the perturbation theory) of the C/E is obtained. Still, C/E results for most isotopes are within about $\pm 10\%$. For Cs-133, Mo-95 and Tc-99, however, the C/E ratios reach values up to about 2. This is consistent with the findings of CHANDA WP12.1, where it was found that the KPERT card sometimes failed to provide accurate results.

Overall, discarding the results of the KPERT card, it can be concluded that a good agreement between the measured and calculated results (C/E discrepancies $< 10\%$) is obtained for all the fission product samples measured at the MINERVE reactor during the CERES program. No significant difference between nuclear data libraries has been observed.

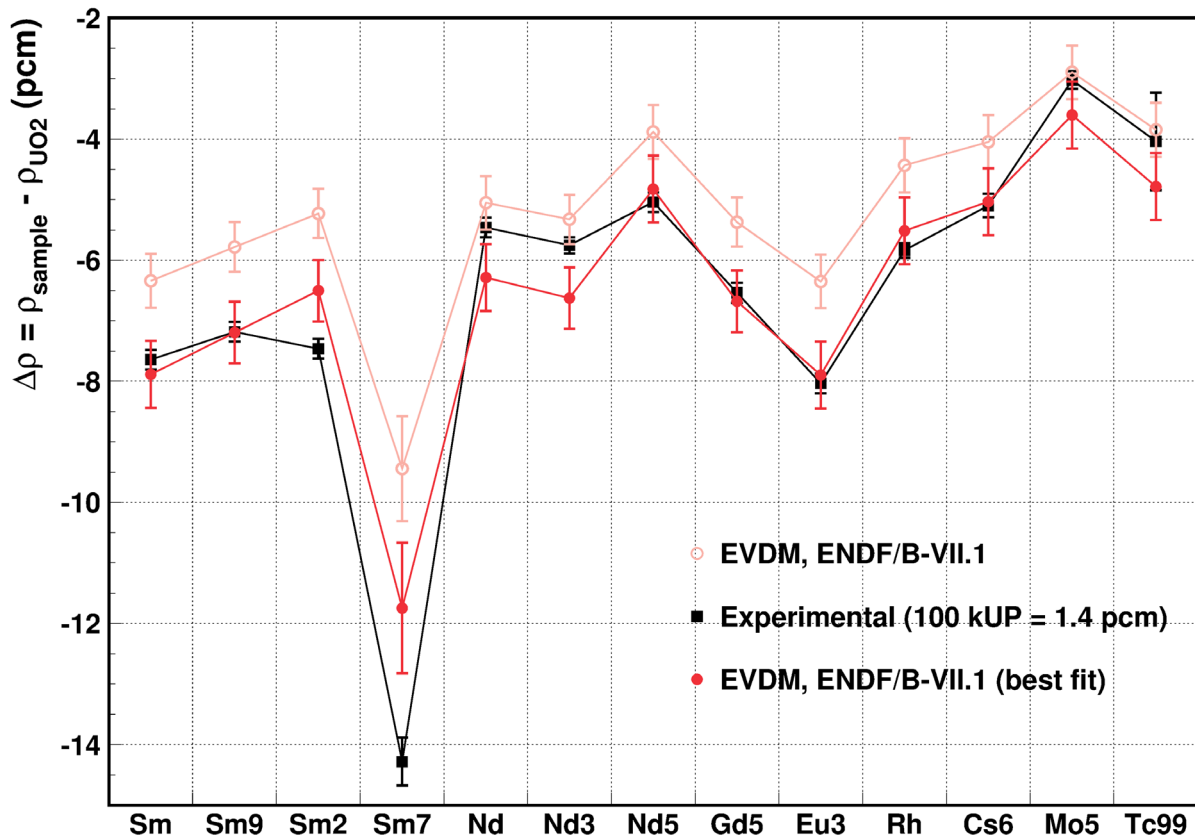


Figure 11. EVDM results (MCNP6.2 and ENDF/B-VII.1) vs. experimental measurements.

Table 10. EVDM results (MCNP6.2 and ENDF/B-VII.1) vs. experimental measurements.

Sample name	Isotope	EVDM, absolute	EVDM, fit to exp.	C/E
Sm	Sm nat.	-6.34 ± 0.44	-7.89 ± 0.55	1.03 ± 0.08
Sm9	Sm-149	-5.78 ± 0.41	-7.19 ± 0.51	1.00 ± 0.07
Sm2	Sm-152	-5.23 ± 0.41	-6.50 ± 0.51	0.87 ± 0.07
Sm7	Sm-147	-9.44 ± 0.87	-11.7 ± 1.1	0.82 ± 0.08
Nd	Nd nat.	-5.05 ± 0.44	-6.29 ± 0.55	1.15 ± 0.11
Nd3	Nd-153	-5.32 ± 0.41	-6.62 ± 0.51	1.15 ± 0.09
Nd5	Nd-155	-3.88 ± 0.44	-4.83 ± 0.55	0.96 ± 0.11
Gd5	Gd-155	-5.37 ± 0.41	-6.68 ± 0.51	1.02 ± 0.08
Eu3	Eu-153	-6.35 ± 0.44	-7.90 ± 0.55	0.98 ± 0.07
Rh	Rh-103	-4.43 ± 0.44	-5.51 ± 0.55	0.94 ± 0.10
Cs6	Cs-133	-4.05 ± 0.44	-5.03 ± 0.55	0.99 ± 0.11
Mo5	Mo-95	-2.90 ± 0.44	-3.60 ± 0.55	1.19 ± 0.19
Tc99	Tc-99	-3.85 ± 0.44	-4.78 ± 0.55	1.18 ± 0.27

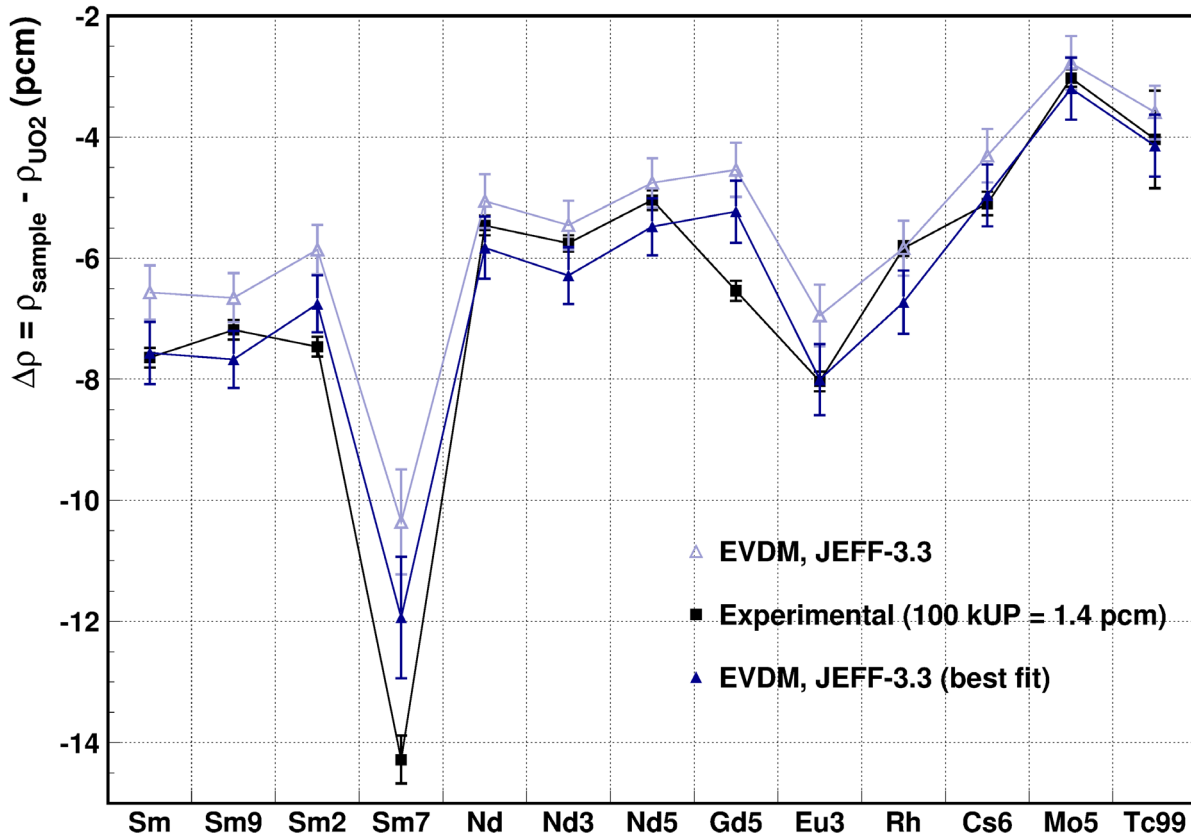


Figure 12. EVDM results (MCNP6.2 and JEFF-3.3) vs. experimental measurements.

Table 11. EVDM results (MCNP6.2 and JEFF-3.3) vs. experimental measurements.

Sample name	Isotope	EVDM, absolute	EVDM, fit to exp.	C/E
Sm	Sm nat.	-6.56 ± 0.45	-7.57 ± 0.51	0.99 ± 0.07
Sm9	Sm-149	-6.65 ± 0.41	-7.67 ± 0.47	1.07 ± 0.07
Sm2	Sm-152	-5.86 ± 0.41	-6.75 ± 0.47	0.91 ± 0.07
Sm7	Sm-147	-10.36 ± 0.87	-11.9 ± 1.0	0.84 ± 0.07
Nd	Nd nat.	-5.06 ± 0.45	-5.83 ± 0.51	1.07 ± 0.10
Nd3	Nd-153	-5.45 ± 0.41	-6.29 ± 0.47	1.09 ± 0.09
Nd5	Nd-155	-4.76 ± 0.41	-5.48 ± 0.47	1.09 ± 0.10
Gd5	Gd-155	-4.54 ± 0.44	-5.23 ± 0.51	0.80 ± 0.08
Eu3	Eu-153	-6.94 ± 0.51	-8.00 ± 0.59	1.00 ± 0.08
Rh	Rh-103	-5.84 ± 0.45	-6.72 ± 0.52	1.15 ± 0.09
Cs6	Cs-133	-4.31 ± 0.44	-4.96 ± 0.51	0.97 ± 0.11
Mo5	Mo-95	-2.78 ± 0.44	-3.20 ± 0.51	1.06 ± 0.18
Tc99	Tc-99	-3.59 ± 0.44	-4.14 ± 0.51	1.03 ± 0.24

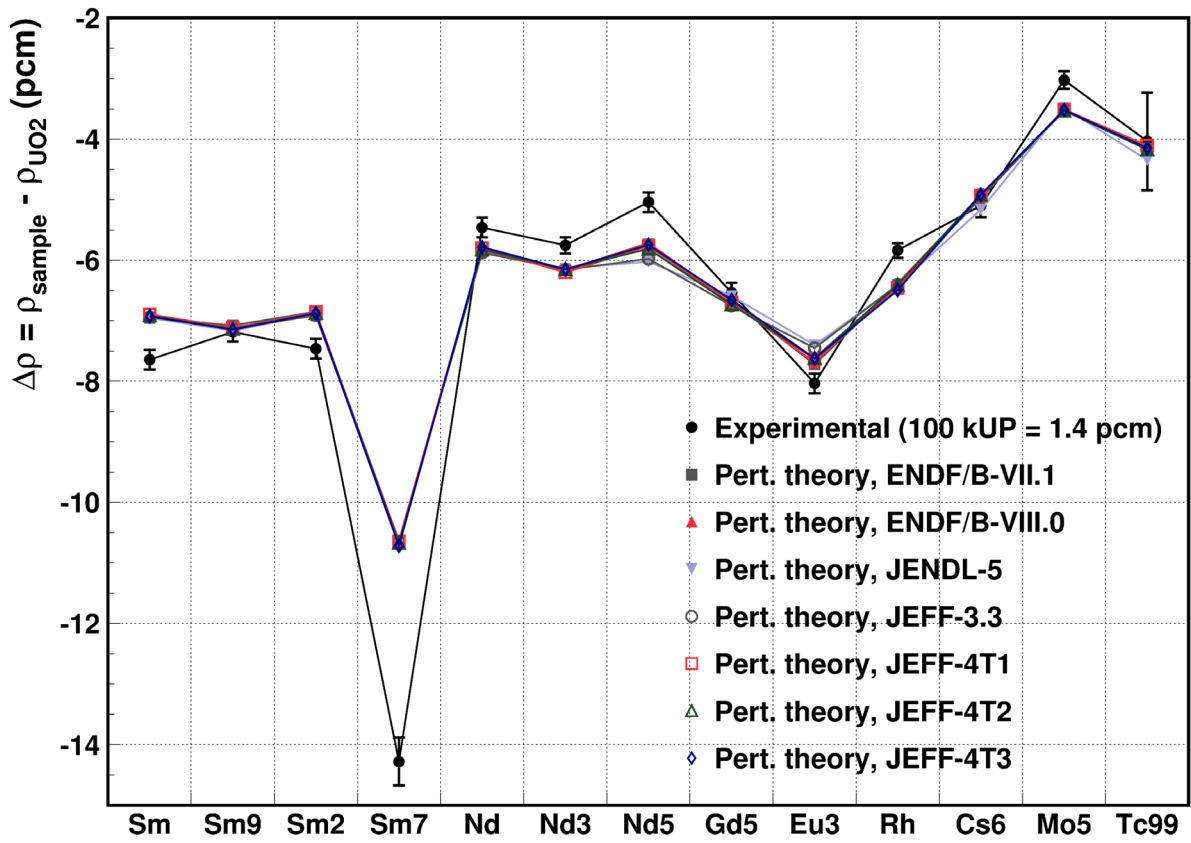


Figure 13. Perturbation theory vs. experimental measurements.

Table 12. Perturbation theory vs. experimental measurements.

Sample name	Isotope	ENDF/B 7.1	ENDF/B 8.0	JENDL 5	JEFF 3.3	JEFF 4T1	JEFF 4T2	JEFF 4T3
Sm	Sm nat.	0.91±0.02	0.91±0.02	0.91±0.02	0.91±0.02	0.90±0.02	0.91±0.02	0.91±0.02
Sm9	Sm-149	0.99±0.02	0.99±0.02	1.00±0.02	0.99±0.02	0.99±0.02	0.99±0.02	1.00±0.02
Sm2	Sm-152	0.92±0.02	0.93±0.02	0.92±0.02	0.93±0.02	0.92±0.02	0.92±0.02	0.92±0.02
Sm7	Sm-147	0.75±0.02	0.74±0.02	0.75±0.02	0.75±0.02	0.75±0.02	0.75±0.02	0.75±0.02
Nd	Nd nat.	1.07±0.03	1.07±0.03	1.07±0.03	1.08±0.03	1.06±0.03	1.07±0.03	1.06±0.03
Nd3	Nd-153	1.07±0.03	1.07±0.03	1.07±0.02	1.07±0.02	1.08±0.03	1.07±0.02	1.07±0.02
Nd5	Nd-155	1.14±0.04	1.13±0.04	1.20±0.04	1.19±0.04	1.14±0.04	1.15±0.04	1.14±0.04
Gd5	Gd-155	1.02±0.03	1.02±0.03	1.08±0.03	1.03±0.03	1.03±0.03	1.03±0.03	1.02±0.03
Eu3	Eu-153	0.96±0.02	0.96±0.02	0.92±0.02	0.93±0.02	0.95±0.02	0.95±0.02	0.95±0.02
Rh	Rh-103	1.10±0.02	1.09±0.02	1.10±0.02	1.10±0.02	1.11±0.02	1.10±0.02	1.11±0.02
Cs6	Cs-133	0.98±0.04	0.97±0.04	1.01±0.04	0.96±0.04	0.97±0.04	0.97±0.04	0.97±0.04
Mo5	Mo-95	1.17±0.06	1.16±0.06	1.15±0.06	1.17±0.06	1.16±0.06	1.17±0.06	1.16±0.06
Tc99	Tc-99	1.03±0.20	1.02±0.21	1.08±0.21	1.03±0.20	1.02±0.20	1.03±0.21	1.03±0.20

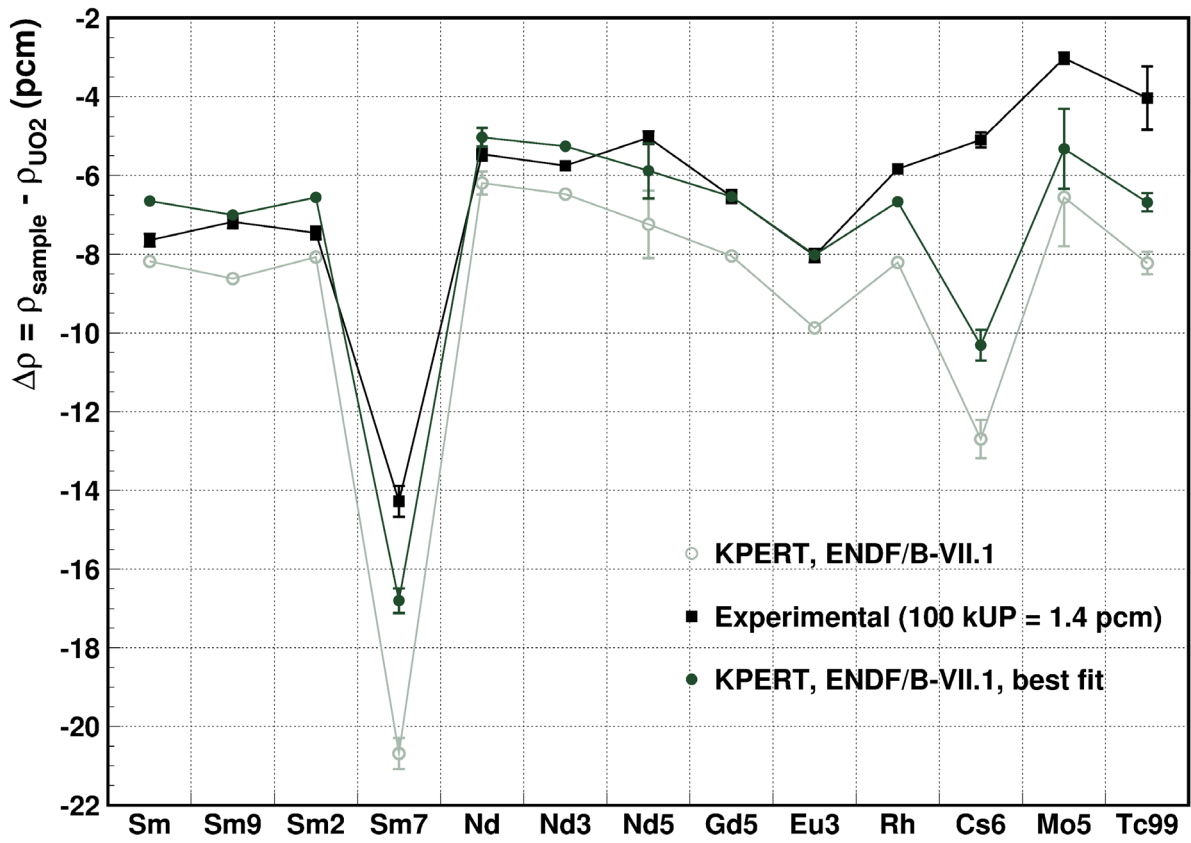


Figure 14. KPERT results (MCNP6.2 and ENDF/B-VII.1) vs. experimental measurements.

Table 13. KPERT results (MCNP6.2 and ENDF/B-VII.1, 10 inactive cycles).

Sample name	Isotope	KPERT	KPERT, fit to exp.	C/E
Sm	Sm nat.	-8.19 ± 0.08	-6.65 ± 0.06	0.87 ± 0.02
Sm9	Sm-149	-8.62 ± 0.08	-7.00 ± 0.07	0.98 ± 0.02
Sm2	Sm-152	-8.07 ± 0.08	-6.56 ± 0.06	0.88 ± 0.02
Sm7	Sm-147	-20.69 ± 0.39	-16.80 ± 0.31	1.18 ± 0.04
Nd	Nd nat.	-6.19 ± 0.29	-5.03 ± 0.24	0.92 ± 0.05
Nd3	Nd-153	-6.47 ± 0.14	-5.26 ± 0.12	0.91 ± 0.03
Nd5	Nd-155	-7.24 ± 0.86	-5.89 ± 0.70	1.17 ± 0.14
Gd5	Gd-155	-8.04 ± 0.09	-6.53 ± 0.07	1.00 ± 0.03
Eu3	Eu-153	-9.87 ± 0.09	-8.02 ± 0.08	1.00 ± 0.02
Rh	Rh-103	-8.21 ± 0.13	-6.67 ± 0.10	1.14 ± 0.03
Cs6	Cs-133	-12.70 ± 0.48	-10.31 ± 0.39	2.02 ± 0.11
Mo5	Mo-95	-6.55 ± 1.25	-5.32 ± 1.01	1.76 ± 0.35
Tc99	Tc-99	-8.23 ± 0.29	-6.68 ± 0.23	1.66 ± 0.33

8.5. Summary and conclusions

The impact in the reactivity of several samples containing a total of 13 relevant fission products measured at the MINERVE reactor has been calculated with three different methodologies: a modified Eigenvalue Difference Method (EVDM) adapted to small reactivity differences, the adjoint weighted perturbation technique with an adjoint flux calculated with MCNP, and the KPERT card of MCNP. When only relative differences between the reactivity effect of the samples are considered (which is the usual procedure in reactivity oscillation technique), both the EVDM and perturbation theory provide C/E ratios within typically about $\pm 10\%$ (up to $\pm 20\%$), for all the measured isotopes. No significant differences between nuclear data libraries have been observed. MCNP KPERT card, for its part, was also capable to provide relative C/E ratios within about $\pm 10\%$, for most the measured isotopes, but failed in some cases (Cs-133, Mo-95 and Tc-99), the C/E ratios reaching a up to about a factor of 2.

8.6. Acknowledgements

This work has been supported by the SANDA project (Grant Agreement Number 847552) of the Euratom Research and Innovation Programme and by the ENRESA-CIEMAT agreement “*Tecnologías Disponibles para la Transmutación de Radionucleidos de Vida Larga*”. The IRPhE database has been obtained through NEA Computer Program Services and MCNP 6.2 has been obtained through RSICC. We are also grateful to We are also grateful to Juan Blázquez Martínez (CIEMAT) for the careful revision of the manuscript and his valuable comments.

8.7. References

- [Bigan 2010] G. Bigan *et al.*, Reactor Physics Experiments on Zero Power Reactors. In D. G. Cacuci (Ed.), *Handbook of Nuclear Engineering*, Springer (2010).
- [Brown 2018] D. A. Brown *et al.*, ENDF/B-VIII.0: *The 8th Major Release of the Nuclear Reaction Data Library with CIELO-project Cross Sections, New Standards and Thermal Scattering Data*. Nuclear Data Sheets 148 (2018) 1-142. DOI: 10.1016/j.nds.2018.02.001.
- [Chadwick 2011] M. B. Chadwick *et al.*, ENDF/B-VII.1 *Nuclear Data for Science and Technology: Cross Sections, Covariances, Fission Product Yields and Decay Data*. Nuclear Data Sheets 112 (2011) 2887-2996. DOI: 10.1016/j.nds.2011.11.002.
- [CERN 1995] CERN’s Computing and Networks Division / Application Software Group. *Physics Analysis Workstation. An Introductory Tutorial*. CERN Program Library Long Writeup Q121 (1995).
- [Dean 2007] C. J. Dean *et al.*, *Validation of important fission product evaluations through CERES integral benchmarks*. In proceedings of the International Conference on Nuclear Data for Science and Technology 2007, 829-832. DOI: 10.1051/ndata:07172.
- [Fougeras 2005] P. Fougeras *et al.*, *The place of EOLE, MINERVE and MASURCA facilities in the R&D Activities of the CEA*. In IGORR 10, Gaithersburg (USA) 12-16 September 2005.
- [Iwamoto 2023] O. Iwamoto *et al.*, *Japanese evaluated nuclear data library version 5: JENDL-5*. Journal of Nuclear Science and Technology 60 (2023) 1-60. DOI: 10.1080/00223131.2022.2141903.
- [James 1994] F. James, *MINUIT – Function Minimization and Error Analysis. Reference Manual Version 94.1*. CERN Program Library entry D506 (1994).
- [Leconte 2017] P. Leconte *et al.*, *New integral/microscopic experiments using common samples*. EU FP7 CHANDA project (GA ID: 605203) deliverable 12.1 (December 2017).

[Noguere 2023] G. Noguere *et al.*, *Time-of-flight measurements of MINERVE samples containing fission products and neutron absorbing isotopes*. EPJ Web of Conferences 284 (2023) 01035. DOI: 10.1051/epjconf/202328401035.

[Panizo 2024] S. Panizo *et al.*, *Sensitivity and uncertainty analyses for advanced nuclear systems (ALFRED, ASTRID, ESR and MYRRHA)*. Progress in Nuclear Energy 172 (2024) 105207. DOI: 10.1016/j.pnucene.2024.105207.

[Perret 2004] G. Perret *et al.*, *Modeling report of the CEA Cadarache MINERVE reactor for the OSMOSE project*. Argonne National Laboratory Report ANL-04/18 (December 2004).

[Plompen 2020] A. J. M. Plompen *et al.*, *The joint evaluated fission and fusion nuclear data library, JEFF-3.3*. European Physical Journal A 56 (2020) 181. DOI: 10.1140/epja/s10050-020-00141-9.

[Santamarina 2007] A. Santamarina and N. Hfaiedh, *The SHEM energy mesh for accurate fuel depletion and BUC calculations*. In International Conference on Nuclear Criticality-Safety (ICNC 2007), St. Petersburg (Russia) 28 May – 1 June 2007.

[Santamarina 2014] A. Santamarina *et al.*, *Reactivity Worth Measurement of Major Fission Products in MINERVE LWR Lattice Experiment*. Nuclear Science and Engineering 178 (2014) 562-581. DOI: 10.13182/NSE14-50.

[Santamarina 2016] A. Santamarina, *Reactivity Worth Measurement of Major Fission Products in MINERVE LWR Lattice Experiment*. MINERVE-FUND-RESR-001. In International Handbook of Evaluated Reactor Physics Benchmark Experiments (IRPhE), OECD/NEA document no. 7496 (July 2019).

[Werner 2017] C. J. Werner (Ed.), *MCNP User's Manual. Code Version 6.2*. Los Alamos National Laboratory Report LA-UR-17-29981 (October 2017).

8.8. Annex: adjoint flux calculation with MCNP

The application of the perturbation theory requires the knowledge of the adjoint flux. The calculation of adjoint fluxes with Monte Carlo codes is a complex issue and therefore its calculation is usually performed with deterministic codes. In particular, adjoint flux calculation is not a standard feature of MCNP. Nevertheless, in this work we have attempted the calculation of the adjoint flux with MCNP using its physical interpretation as neutron importance, i. e. interpreting $\Phi_0^\dagger(\vec{r}, E)$ as the total progeny of a neutron born at position \vec{r} with energy E .

With this calculation scheme, the adjoint flux $\Phi_0^\dagger(\vec{r}, E)$ is obtained as the total number of neutrons produced from a fixed source calculation (i.e. not an eigenvalue calculation) with a neutron source placed at position \vec{r} (for this work, we have considered a source distributed within the sample cell) and emitting neutrons of energy E (for this work, we have considered the 281-energy group SHEM structure also used in [Santamarina 2014]). In this way the adjoint flux is obtained except for an arbitrary normalization factor, e.g. a factor so that its integral value over the entire range is 1.

An advantage of this calculation scheme is that since it takes into account the neutrons produced in the whole reactor, a large statistics can be accumulated and therefore is very efficient in terms of computational resources. On the other hand, an issue with this scheme is that it cannot be applied to a critical reactor, since it will result in infinite neutron chains. Even in subcritical systems very close to criticality very long neutron histories will occur, that in turn will result in oscillating results or even calculation failure. For this reason, the adjoint flux has been calculated in a subcritical (but close to critical) model of the MINERVE core obtained by inserting the control rods. Notice that the lower the value of the criticality, the lower will be the number of long neutron histories and hence the lower the risks to have oscillating solutions or calculation failures, as stated above, but, on the other hand, there

is a risk of introducing a bias in the results (as we are calculating the adjoint flux in a system more different from the critical state).

The results obtained with this technique, for both reference samples UF and UC, are listed in Table 14. The values listed are the total number of neutrons produced in the whole system after the introduction of 5×10^4 or 1×10^5 neutrons in the system, depending on the case, as indicated in the title row. For the case of the UF sample, results obtained with the control rods at two different positions, corresponding $k_{eff}=0.975$ and 0.987 , are also shown. These calculations have been performed to determine the optimal level of subcriticality for calculating the adjoint flux, as discussed above. The results are shown graphically in Figure 15, normalized so that its integrated value is 1 in all cases. It can be observed that the results obtained are virtually the same, which means that the subcriticality level, if it is small, has a low impact in the adjoint flux calculation. The adjoint-weighted results presented in this work were all calculated with the adjoint flux obtained with $k_{eff} = 0.987$, the higher criticality value of the two calculations performed.

In the figure, deterministic results obtained with the APOLLO2 (in a more simplified reactor model) code also provided in [Santamarina 2016] are also plotted alongside for comparison (with the same normalization); a very good agreement can be observed.

It may be worthwhile to comment that the values of the neutron multiplication listed in Table 14 are much higher than the ones obtained with the well-known formula for the total neutron progeny $k_{eff}/(1 - k_{eff})$. For $k_{eff} = 0.987$ this formula would result in $k_{eff}/(1 - k_{eff}) \approx 76$, while, for example the number of total number of neutrons produced in the system for the case of the UF sample , $k_{eff}=0.987$, initial neutron energy $E < 2.5 \times 10^9$ MeV is $32271534/50000 \approx 645$. This discrepancy is a consequence of the source position having a very high source importance, see for instance [Gandini 2002].

As a final comment, the statistical errors are very small, given the large statistics accumulated with this method. This causes that the differences between the results calculated with the two different values of k_{eff} (even if small) cannot be explained merely by statistical effects. The reason for this discrepancy is unknown, a possible explanation is the presence of very long neutron stories as the systems approaches criticality.

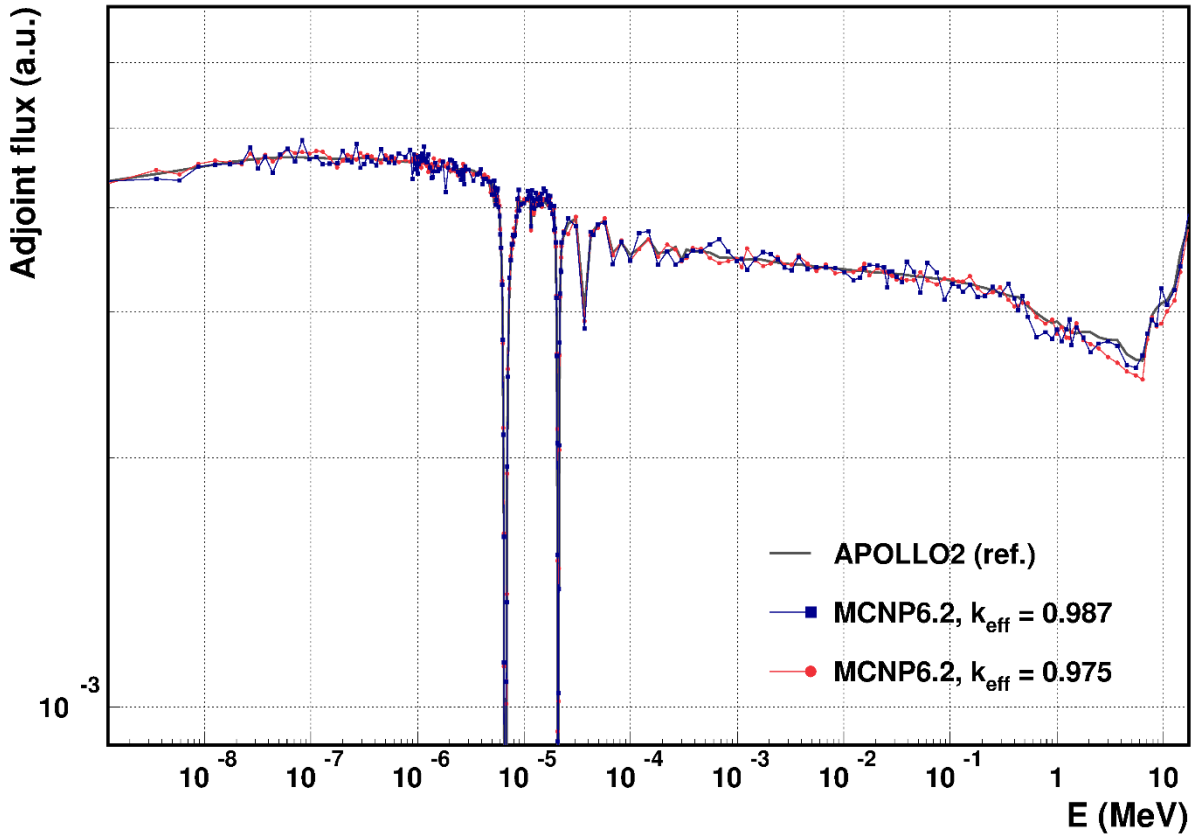


Figure 15. Calculated adjoint flux spectrum in the simple cell (UF) at two different levels of subcriticality. APOLLO2 results [Santamarina 2016] are also plotted for comparison.

Table 14. Total neutron production in the MINERVE system due the introduction of a number of source neutrons (s. n.) in the oscillation sample position, for two different samples (UF and UC). For the case of the UC sample, results for two values of the criticality ($k_{eff}=0.975$ and $k_{eff}=0.987$) are listed. The number of initial source neutrons is 5×10^4 for $k_{eff}=0.987$ and 1×10^5 for $k_{eff}=0.975$.

E_{min} (MeV)	E_{max} (MeV)	UF, $k_{eff}=0.975$ ($1E+05$ s. n.)	UF, $k_{eff}=0.987$ ($5E+04$ s. n.)	UC, $k_{eff}=0.987$ ($5E+04$ s. n.)
0.00E+00	2.50E-09	32490088	32271534	32672230
2.50E-09	4.56E-09	33759595	32487317	33331072
4.56E-09	7.15E-09	33350205	32361671	34891123
7.15E-09	1.05E-08	34314300	33589396	35475550
1.05E-08	1.48E-08	34624345	33806518	36279833
1.48E-08	2.00E-08	34450330	33851877	33469989
2.00E-08	2.49E-08	34284480	33968968	34098167
2.49E-08	2.93E-08	35294317	35443693	34869484
2.93E-08	3.44E-08	34490715	33443666	35107426
3.44E-08	4.03E-08	35208069	34542076	35321744
4.03E-08	4.73E-08	34581158	33045001	33698973
4.73E-08	5.55E-08	34946533	34757672	35438163
5.55E-08	6.52E-08	35775380	35337729	34010956
6.52E-08	7.65E-08	35360472	34104860	33869900
7.65E-08	8.98E-08	35494739	36194269	35383656
8.98E-08	1.04E-07	35291731	34321581	34574075
1.04E-07	1.20E-07	35587171	34503182	36127497
1.20E-07	1.38E-07	35505832	33822875	34831508

1.38E-07	1.62E-07	34899619	33892417	35619718
1.62E-07	1.90E-07	33997115	33938198	34611698
1.90E-07	2.10E-07	34650125	35155228	34747125
2.10E-07	2.31E-07	35204078	34217100	33852843
2.31E-07	2.55E-07	35019111	34001990	35289121
2.55E-07	2.80E-07	34747136	35827286	35663351
2.80E-07	3.05E-07	35370617	33502878	34255034
3.05E-07	3.25E-07	35006889	33881842	35071010
3.25E-07	3.53E-07	35196396	34524771	34151820
3.53E-07	3.90E-07	35071756	34087434	36398986
3.90E-07	4.32E-07	34789207	33725211	33994327
4.32E-07	4.75E-07	34439318	35283477	34892019
4.75E-07	5.20E-07	35160001	34321590	34218369
5.20E-07	5.55E-07	34870034	33980786	33990204
5.55E-07	5.95E-07	34669762	34552998	34589832
5.95E-07	6.25E-07	34881735	33941326	33774615
6.25E-07	7.20E-07	34487895	34878375	34523256
7.20E-07	8.20E-07	34751556	34502215	33968918
8.20E-07	8.80E-07	34542973	35198530	33353843
8.80E-07	9.20E-07	34807718	32472127	34030499
9.20E-07	9.44E-07	34612450	34804859	34623207
9.44E-07	9.64E-07	35238076	33915872	34354726
9.64E-07	9.82E-07	34886111	33357907	34483818
9.82E-07	9.97E-07	35072934	33832521	33981502
9.97E-07	1.01E-06	34823285	34514062	34618419
1.01E-06	1.02E-06	34618920	32977543	33854027
1.02E-06	1.03E-06	34837149	33846651	35163932
1.03E-06	1.08E-06	34592418	34613874	34664728
1.08E-06	1.09E-06	33989287	34147765	34197226
1.09E-06	1.10E-06	34555700	34750610	32927185
1.10E-06	1.12E-06	34476958	34879495	34455064
1.12E-06	1.13E-06	34483625	34427246	34323647
1.13E-06	1.15E-06	34875852	34212296	33753272
1.15E-06	1.17E-06	34538862	35566701	34290538
1.17E-06	1.21E-06	34316406	34362897	36292878
1.21E-06	1.25E-06	34136990	34021566	34607856
1.25E-06	1.29E-06	33577366	34769894	34378209
1.29E-06	1.33E-06	34003903	33534100	34584873
1.33E-06	1.38E-06	34295771	32578781	34415055
1.38E-06	1.41E-06	33697690	32653346	33981055
1.41E-06	1.44E-06	34834057	33162307	33364297
1.44E-06	1.52E-06	34251916	33975959	35452349
1.52E-06	1.59E-06	34013380	33178925	33615249
1.59E-06	1.67E-06	34653636	33403086	33056376
1.67E-06	1.78E-06	34613654	34087087	34515510
1.78E-06	1.90E-06	34087886	31318196	34218753
1.90E-06	1.99E-06	34378307	33497002	34148571
1.99E-06	2.07E-06	33736421	34287152	32110452
2.07E-06	2.16E-06	33665604	34220182	34145061
2.16E-06	2.22E-06	34313950	33388830	34146453
2.22E-06	2.27E-06	33870930	33929451	33283235
2.27E-06	2.33E-06	33623572	33582767	33144994
2.33E-06	2.47E-06	33261899	33132297	33709194
2.47E-06	2.55E-06	33481412	32900956	31364789
2.55E-06	2.59E-06	33349198	32398292	34371859

2.59E-06	2.62E-06	33699749	32818286	33497771
2.62E-06	2.64E-06	33817927	33278546	32370547
2.64E-06	2.70E-06	34330732	33269012	33541696
2.70E-06	2.72E-06	33199525	32484679	34365727
2.72E-06	2.74E-06	34170644	33292467	32817934
2.74E-06	2.78E-06	33626493	32000154	32915368
2.78E-06	2.88E-06	33663010	33648092	33525472
2.88E-06	3.14E-06	33784282	33332402	33023799
3.14E-06	3.54E-06	33351715	32306799	32798297
3.54E-06	3.71E-06	33384504	32908535	32682377
3.71E-06	3.88E-06	33543679	32988909	33901900
3.88E-06	4.00E-06	33746141	33411565	31589674
4.00E-06	4.22E-06	33094571	31980620	32729467
4.22E-06	4.31E-06	33326715	32487511	33149871
4.31E-06	4.42E-06	32916909	32520992	33352052
4.42E-06	4.77E-06	33090097	32290348	32965762
4.77E-06	4.93E-06	31736386	32212479	32234526
4.93E-06	5.11E-06	31904253	31117772	32563636
5.11E-06	5.21E-06	31407290	31108934	30903276
5.21E-06	5.32E-06	32215148	32326000	31247451
5.32E-06	5.38E-06	32136669	31731401	31244843
5.38E-06	5.41E-06	31332959	31512662	32800393
5.41E-06	5.49E-06	30859554	30224823	32009491
5.49E-06	5.53E-06	31543150	30632003	30360092
5.53E-06	5.62E-06	31368102	31457887	31455722
5.62E-06	5.72E-06	31063261	31656566	31972969
5.72E-06	5.80E-06	30942346	30053079	31039231
5.80E-06	5.96E-06	30569345	29294701	30603394
5.96E-06	6.06E-06	28619000	27833681	28946041
6.06E-06	6.16E-06	27126845	26846569	28210760
6.16E-06	6.28E-06	24815811	24228192	25474627
6.28E-06	6.36E-06	20841460	20785784	23446388
6.36E-06	6.43E-06	16479266	15959111	18624119
6.43E-06	6.48E-06	12294995	12016167	15335568
6.48E-06	6.51E-06	8493681	8477240	12343394
6.51E-06	6.54E-06	5679010	5465841	8699538
6.54E-06	6.56E-06	3961890	3728499	6124170
6.56E-06	6.57E-06	2514153	2261391	4016420
6.57E-06	6.59E-06	1711460	1704811	2599289
6.59E-06	6.61E-06	973524	1069240	1704431
6.61E-06	6.63E-06	679881	614835	967836
6.63E-06	6.72E-06	361509	388347	558601
6.72E-06	6.74E-06	524405	702724	833466
6.74E-06	6.76E-06	932048	825306	1261667
6.76E-06	6.78E-06	1405649	1246898	2203662
6.78E-06	6.79E-06	2096577	2157111	3763082
6.79E-06	6.81E-06	3372452	3538257	5352021
6.81E-06	6.84E-06	5521802	5100383	8266494
6.84E-06	6.87E-06	7662049	8033734	10960470
6.87E-06	6.92E-06	10392511	10019478	14739429
6.92E-06	6.99E-06	14517145	14615244	18208858
6.99E-06	7.14E-06	19421195	18739712	21456289
7.14E-06	7.38E-06	24271347	24702822	25550407
7.38E-06	7.60E-06	26576898	25936224	26898669
7.60E-06	7.74E-06	27104331	27101730	27965521

7.74E-06	7.84E-06	28046228	27067251	28581102
7.84E-06	7.97E-06	27570075	27785488	28648210
7.97E-06	8.13E-06	28717987	27716742	30286973
8.13E-06	8.30E-06	28397772	27826882	29723372
8.30E-06	8.52E-06	29281892	29273097	30529769
8.52E-06	8.67E-06	30129493	29270443	29804269
8.67E-06	8.80E-06	31018657	30753359	31313395
8.80E-06	8.98E-06	31242457	31532973	31078273
8.98E-06	9.14E-06	30731132	29737161	30896293
9.14E-06	9.50E-06	30610093	30285433	30175570
9.50E-06	1.06E-05	31093086	30362649	31344812
1.06E-05	1.08E-05	31026687	30701363	30975748
1.08E-05	1.11E-05	31093361	31430906	30394312
1.11E-05	1.13E-05	31313298	30961080	30831363
1.13E-05	1.16E-05	31155202	31087350	30456322
1.16E-05	1.17E-05	28539771	28475532	28456203
1.17E-05	1.18E-05	30064340	30020853	29775570
1.18E-05	1.20E-05	30502338	31471561	30019616
1.20E-05	1.21E-05	31148423	30778071	31496126
1.21E-05	1.23E-05	31055288	30624533	30297365
1.23E-05	1.25E-05	29865729	30580974	29728207
1.25E-05	1.26E-05	30137488	29886513	30187511
1.26E-05	1.33E-05	30752231	31244154	31388475
1.33E-05	1.35E-05	31454220	30728871	31823926
1.35E-05	1.40E-05	31226395	30198101	31173215
1.40E-05	1.43E-05	31598693	30901042	30982131
1.43E-05	1.45E-05	31490932	30703131	30172504
1.45E-05	1.46E-05	30764397	30270135	30722427
1.46E-05	1.47E-05	30857251	30256463	30698679
1.47E-05	1.49E-05	30479269	31200940	31445525
1.49E-05	1.58E-05	31168347	31650526	31264479
1.58E-05	1.60E-05	31090379	31397058	30609238
1.60E-05	1.66E-05	31074006	30678443	30160130
1.66E-05	1.68E-05	31091035	31037277	30657562
1.68E-05	1.74E-05	30559718	30475112	30963978
1.74E-05	1.76E-05	30787498	29988376	30118875
1.76E-05	1.78E-05	31238286	30974153	30528860
1.78E-05	1.80E-05	30660687	30297692	30865117
1.80E-05	1.91E-05	30068937	29445285	30324707
1.91E-05	1.92E-05	29557099	28187577	29795678
1.92E-05	1.94E-05	30347963	30144298	29872452
1.94E-05	1.96E-05	28400270	28316904	30309174
1.96E-05	2.01E-05	27282287	27229546	27855645
2.01E-05	2.03E-05	23818806	23354734	26015075
2.03E-05	2.04E-05	20276680	19869085	22191990
2.04E-05	2.05E-05	16430924	15576324	18376902
2.05E-05	2.06E-05	11402437	11426926	14468077
2.06E-05	2.07E-05	7092534	6806005	9844855
2.07E-05	2.08E-05	4087666	4319960	5346989
2.08E-05	2.10E-05	2268566	1771758	3049080
2.10E-05	2.11E-05	1842784	1715192	2519261
2.11E-05	2.11E-05	4319984	4117368	5873321
2.11E-05	2.12E-05	7713008	7785569	11035505
2.12E-05	2.13E-05	11148006	10394049	14954071
2.13E-05	2.15E-05	15506960	15498853	17622137

2.15E-05	2.17E-05	20167749	20616514	22469164
2.17E-05	2.20E-05	23704200	23609599	25426726
2.20E-05	2.22E-05	25497557	25203770	27475161
2.22E-05	2.24E-05	26476593	25088642	28221459
2.24E-05	2.25E-05	27315025	27235615	27591066
2.25E-05	2.46E-05	28465937	27978731	29291229
2.46E-05	2.76E-05	28256614	29092099	29112891
2.76E-05	3.37E-05	29626755	28503796	29703115
3.37E-05	4.02E-05	22175224	21426695	24044189
4.02E-05	4.40E-05	28144901	28046635	27782571
4.40E-05	4.58E-05	28446800	27799541	28948119
4.58E-05	5.27E-05	28741620	28595697	28281586
5.27E-05	6.14E-05	29531426	28782674	28472156
6.14E-05	7.50E-05	26620543	25637077	25490462
7.50E-05	8.90E-05	27745243	27304873	27065809
8.90E-05	1.09E-04	26211864	25872714	26438410
1.09E-04	1.33E-04	27091346	27954142	27505991
1.33E-04	1.62E-04	27826835	28106708	27713028
1.62E-04	1.98E-04	26486264	25606600	26217640
1.98E-04	2.42E-04	27444744	26555910	27213341
2.42E-04	2.84E-04	27048500	25609656	27578402
2.84E-04	3.20E-04	26184831	25949021	25962142
3.20E-04	3.54E-04	26425514	26224428	26951709
3.54E-04	4.11E-04	27157728	26631715	27426006
4.11E-04	5.02E-04	27107281	26553987	27398814
5.02E-04	6.13E-04	26422244	27070635	25796851
6.13E-04	7.49E-04	26064838	27479170	26354247
7.49E-04	9.08E-04	26215917	26549378	27246517
9.08E-04	1.06E-03	26371137	25858136	25990790
1.06E-03	1.14E-03	25760119	26005836	26363179
1.14E-03	1.35E-03	27151357	25240382	25715849
1.35E-03	1.61E-03	26256748	26020847	26898005
1.61E-03	1.91E-03	25840518	26524955	26159659
1.91E-03	2.22E-03	26028955	26347355	26751640
2.22E-03	2.58E-03	26508996	25957530	26791856
2.58E-03	3.00E-03	25944418	25386493	26881836
3.00E-03	3.48E-03	25958980	25202159	24602261
3.48E-03	4.10E-03	26620143	26145187	25476964
4.10E-03	5.00E-03	26035496	25278982	24822293
5.00E-03	6.11E-03	25483847	25419950	24891228
6.11E-03	7.47E-03	25945241	25403362	25322893
7.47E-03	9.12E-03	25325727	25380542	25273387
9.12E-03	1.11E-02	25403350	25079729	25268903
1.11E-02	1.36E-02	25418492	24529798	25350599
1.36E-02	1.49E-02	25601440	24679911	25471381
1.49E-02	1.62E-02	26021411	25347210	24582344
1.62E-02	1.86E-02	25186649	25578822	25182946
1.86E-02	2.27E-02	25691355	25520237	25001106
2.27E-02	2.50E-02	25424434	25400557	24091877
2.50E-02	2.61E-02	25403166	24028272	24968465
2.61E-02	2.74E-02	25315115	25126611	24983429
2.74E-02	2.93E-02	25146745	25136921	24519065
2.93E-02	3.35E-02	24888748	24776065	26264977
3.35E-02	3.70E-02	24964208	24380348	24662788
3.70E-02	4.09E-02	24855245	25796001	24845972

4.09E-02	4.99E-02	24862991	25099801	25283161
4.99E-02	5.52E-02	25403238	23678260	24922476
5.52E-02	6.74E-02	24830704	25728107	25632066
6.74E-02	8.23E-02	24554946	25037940	25126458
8.23E-02	9.47E-02	24947406	23214321	25398050
9.47E-02	1.16E-01	24899477	24255740	24968864
1.16E-01	1.23E-01	24758857	24091011	25033040
1.23E-01	1.40E-01	24762639	23731031	25460503
1.40E-01	1.65E-01	25130870	24203094	24857323
1.65E-01	1.95E-01	24322482	23390157	24337300
1.95E-01	2.30E-01	23835232	23481680	24027245
2.30E-01	2.68E-01	24018692	24053321	23440506
2.68E-01	3.21E-01	24368237	23551259	23267098
3.21E-01	3.84E-01	23523421	24267929	23800852
3.84E-01	4.13E-01	23113042	23307003	23130685
4.13E-01	4.56E-01	23137612	22557693	23784534
4.56E-01	4.94E-01	23351434	23468875	22992676
4.94E-01	5.78E-01	23309544	22138223	22981139
5.78E-01	7.07E-01	22417643	20931568	22374843
7.07E-01	8.60E-01	22016216	21219357	22160928
8.60E-01	9.51E-01	22269858	20846309	21035819
9.51E-01	1.05E+00	21404769	21374373	21640953
1.05E+00	1.16E+00	21796886	20698061	21386161
1.16E+00	1.29E+00	21189361	21383362	20948049
1.29E+00	1.34E+00	21158875	21991879	20598175
1.34E+00	1.41E+00	21502190	20462663	21194645
1.41E+00	1.64E+00	22053285	21492303	21404814
1.64E+00	1.90E+00	21031364	20898980	20578508
1.90E+00	2.23E+00	20806954	20070247	21410693
2.23E+00	2.73E+00	20558044	20546588	21153233
2.73E+00	3.33E+00	20064330	20689343	19600632
3.33E+00	4.07E+00	19755756	20422510	20348139
4.07E+00	4.97E+00	19275379	19367662	19412626
4.97E+00	6.07E+00	19068400	19212308	18863664
6.07E+00	6.70E+00	18864018	19899243	19897257
6.70E+00	7.41E+00	21082023	21139219	20448110
7.41E+00	8.19E+00	22407762	21942763	21831793
8.19E+00	9.05E+00	21852791	21647703	22226625
9.05E+00	1.00E+01	22031352	23956366	22002747
1.00E+01	1.16E+01	22796489	22918974	22519170
1.16E+01	1.38E+01	23479856	23841127	22805083
1.38E+01	1.49E+01	25418893	25471113	25681312
1.49E+01	1.96E+01	28715002	29645846	28941064

8.8.1. References for annex

[Gandini 2002] A. Gandini and M. Salvatores, *The Physics of Subcritical Multiplying Systems*. Journal of Nuclear Science and Technology 39 (2002) 673-686. DOI: 10.1080/18811248.2002.9715249.

[Santamarina 2016] A. Santamarina, *Reactivity Worth Measurement of Major Fission Products in MINERVE LWR Lattice Experiment*. MINERVE-FUND-RESR-001. In International Handbook of Evaluated Reactor Physics Benchmark Experiments (IRPhE), OECD/NEA document no. 7496 (July 2019).